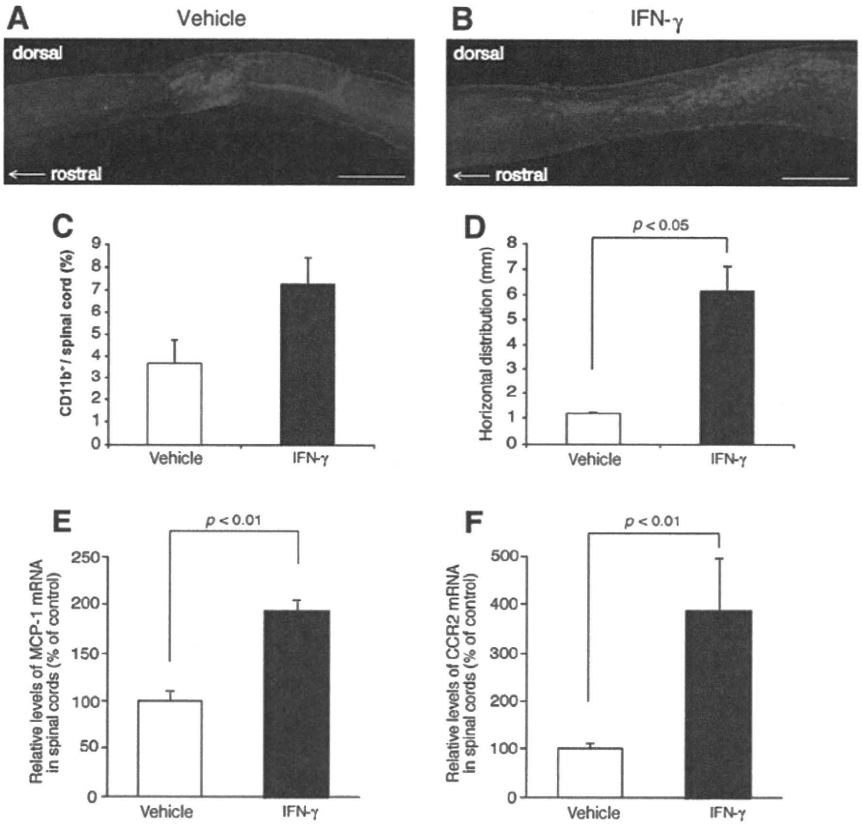

FIG. 3. Horizontal distribution of CD11b-positive macrophages/microglia in IFN-γ-treated mice post-SCI. Ten days post-SCI, the spinal cords of vehicle-treated (**A**) and IFN-γ-treated (**B**) mice were fixed and sagittal sections were stained with anti-CD11b antibody (scale bar = 1 mm). (**C**) The CD11b-positive area in a section including 5 mm rostral and caudal from the epicenter was measured, and is expressed as the percentage of CD11b-positive area relative to the total area examined. There was no statistically significant difference between the vehicle-treated group ($3.7 \pm 1.1\%$), and the IFN-γ-treated group ($7.3 \pm 1.1\%$; $p = 0.08$). (**D**) The length of the horizontal distribution of CD11b-positive cells was measured. Six spinal cord sections per animal and three animals from each group were included in the assessment. There was a statistically significant difference between the vehicle-treated group (1.18 ± 0.03 mm), and the IFN-γ-treated group (6.15 ± 0.96 mm; $p < 0.05$). Quantitative RT-PCR for MCP-1 (**E**) and CCR2 (**F**) was performed by using mRNA isolated from 6-mm-long sections of injured spinal cords including the lesion center at the middle ($n = 3$). Injured spinal cords were dissected 7 days post-SCI (IFN-γ, interferon-γ; SCI, spinal cord injury; RT-PCR, real-time polymerase chain reaction).

IFN-γ treatment decreases the accumulation of CSPG post-SCI

Following SCI, reactive astrocytes accumulate around the epicenter of the injured spinal cord and express molecules that inhibit axonal regeneration. Therefore, we examined the distribution of reactive astrocytes at 10 days post-SCI. Consistent with a previous report (Popovich et al., 1997), reactive astrocytes were detected in the tissue circumscribing the wound cavity at the lesion center (Fig. 4A and B). In the vehicle-treated group, GFAP staining was highest at the lesion edge and sharply decreased rostrally and caudally (Fig. 4A). In contrast, elevated GFAP staining in the IFN-γ-treated group had extended rostrally and caudally (Fig. 4B). Consistent with this observation, quantification of GFAP-positive immunoreactivity revealed that the accumulated reactive astrocytes were significantly higher rostrally and caudally in the IFN-γ-treated group than in the control group, except at the epicenter (Fig. 4C).

Next, we used immunohistochemistry to analyze the expression of CSPGs, which are the major axon growth inhibitors that accumulate following CNS injury, and which are mainly produced by reactive astrocytes (Fig. 5A–D). The CSPG signals were detected around the wound cavity at the epicenter. The distribution of immunoreactivity for CSPGs was similar to that of the GFAP-positive reactive astrocytes, as expected (McKeon et al., 1991, 1999; Smith and Strunz, 2005; Yiu and He, 2006). The mean density of CSPGs was significantly reduced in the IFN-γ-treated group ($0.57 \pm 0.05\%$), compared to the vehicle-treated group ($1.16 \pm 0.07\%$), suggesting that IFN-γ treatment decreased the accumulation of CSPGs following SCI in mice (data not shown). In addition, we measured the horizontal distribution of CSPG expression by quantification of immunoreactivity for CSPG. In the vehicle-treated group, CSPG staining was highest at the lesion edge, and sharply decreased rostrally and caudally (Fig. 5E). In contrast, elevated CSPG staining in the IFN-γ-treated group extended rostrally and caudally (Fig. 5E). Horizontal distribution of CSPG immunoreactivity was similar to that of GFAP (Fig. 4A–E). To directly examine whether the levels of CSPG production were reduced by IFN-γ treatment, we analyzed the mRNA

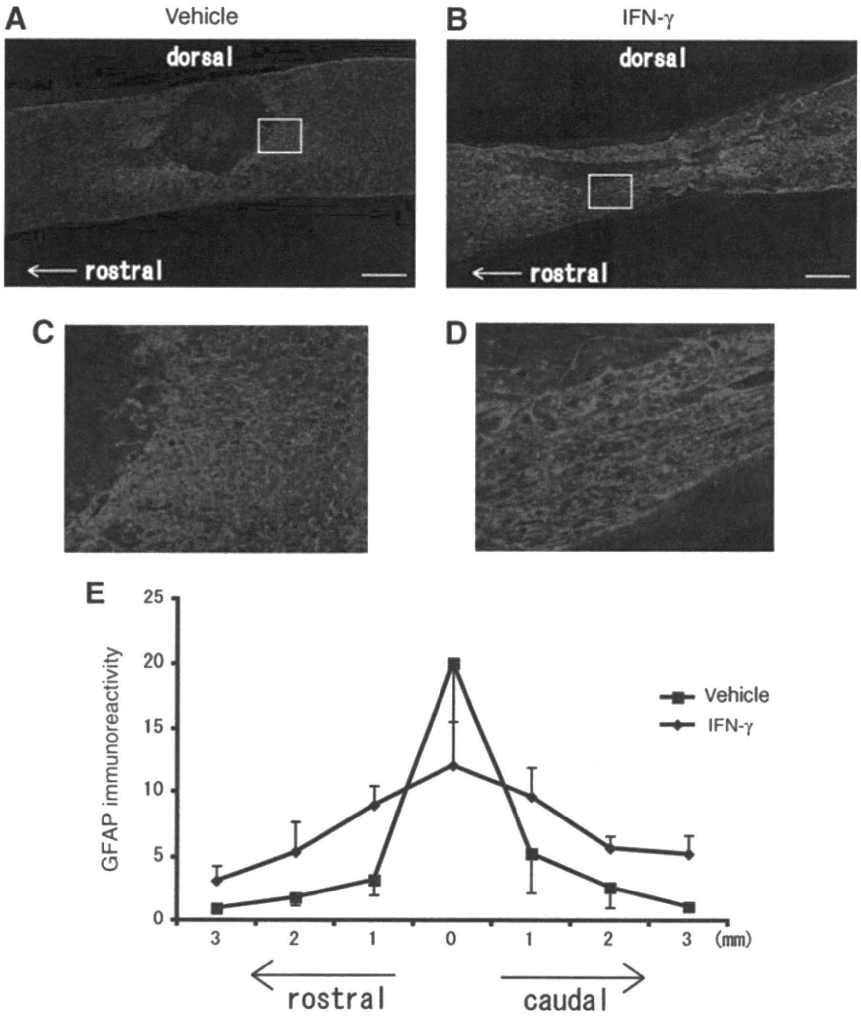

FIG. 4. Accumulation of glial fibrillary acidic protein (GFAP)-positive reactive astrocytes post-SCI. At 10 days post-SCI, the spinal cords of vehicle-treated (**A** and **C**), and IFN-γ-treated (**B** and **D**) mice were fixed and sagittal sections were immunolabeled with anti-GFAP antibody (scale bar = 400 μm). (**E**) The GFAP immunoreactivity was quantified rostrally and caudally from the lesion center at 1-mm intervals, and is expressed as the relative ratio to that of control animals at 3 mm rostral. There was a statistically significant difference between the control group and the IFN-γ-treated group, except at the epicenter ($p < 0.05$; IFN-γ, interferon-γ; SCI, SCI, spinal cord injury).

and protein levels of neurocan, one of the CSPGs that is typically upregulated following CNS injury, in injured spinal cords by quantitative RT-PCR and Western blotting, respectively. IFN-γ treatment significantly reduced the levels of neurocan in the tissues surrounding the lesion epicenter at 7 days post-SCI at both mRNA and protein levels (Fig. 6A and B). Since reactive astrocytes are considered to be a major source of CSPGs post-CNS injury, we evaluated the effects of IFN-γ on neurocan expression by stimulated astrocytes *in vitro* (Fig. 6C and D). It has been reported that TGF-β and EGF enhance the expression of GFAP and neurocan in cultured astrocytes as pathologically relevant stimulators, and mimic the molecular events occurring in reactive astrocytes in the injured spinal cord (Asher et al., 2000; Smith and Strunz, 2005). Therefore, we evaluated the effects of IFN-γ on TGF-β- or EGF-induced expression of neurocan in cultured astrocytes. IFN-γ significantly decreased the levels of neurocan mRNA in TGF-β- or EGF-treated astrocytes (Fig. 6C). In addition, IFN-γ cancelled the TGF-β-induced upregulation of neurocan protein expression, whereas IFN-γ treatment had no influence on TGF-β-induced GFAP expression enhancement (Fig. 6D). However, IFN-γ had no significant effect on EGF-induced neurocan upregulation (data not shown). These data suggest that IFN-γ treatment may block the upregulation of CSPGs in activated astrocytes at the transcriptional level.

IFN-γ had no effect on the levels of other axon growth inhibitors

We analyzed whether IFN-γ modulated the levels of other axon growth inhibitors such as semaphorin 3A and Nogo A, both of which were reported to be upregulated and involved in the deficit of axonal recovery post-SCI, by Western blotting. IFN-γ exhibited no effects on the levels of either protein in injured spinal cords at 5, 10, and 14 days post-SCI (data not shown).

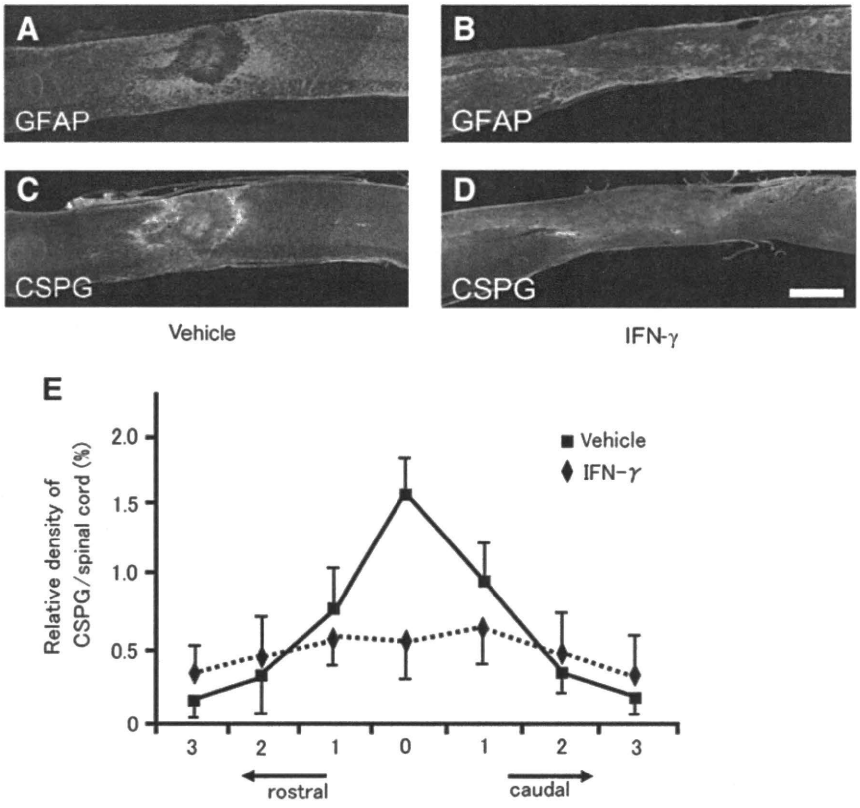

FIG. 5. Interferon-γ (IFN-γ) alters chondroitin sulfate proteoglycan (CSPG) distribution post-SCI. At 10 days post-SCI, the spinal cords of vehicle-treated (**A** and **C**), and IFN-γ-treated (**B** and **D**) mice, were fixed and parasagittal sections were stained with anti-GFAP antibody (**A** and **B**), and anti-CSPG antibody (**C** and **D**; scale bar = 500 μm). Note that the distribution of the CSPG signals (green) is similar to that of the GFAP signals (red). (**E**) Quantification of CSPG expression. The method of measurement was the same as for the quantification of GFAP expression shown in Figure 4E (GFAP, glial fibrillary acidic protein; SCI, spinal cord injury).

IFN-γ treatment increased 5-HT-positive fibers around the epicenter following SCI

Since the serotonergic raphe-spinal neuronal circuit contributes to locomotor function (Kim et al., 2004), we examined serotonergic fiber sprouting by 5-HT immunostaining at 6 weeks post-SCI. Numerous 5-HT-positive fibers were found close to the lesion cavity of injured spinal cords in IFN-γ-treated mice (Fig. 7C and D), whereas few positive fibers were detected in the vehicle-treated mice (Fig. 7A and B). The number of fibers was counted at 1-mm intervals rostrally or caudally from the lesion center. The number of 5-HT-positive fibers was significantly higher at the center and 1 mm rostral to the lesion center in the IFN-γ-treated group ($p < 0.05$) (Fig. 7E), suggesting that IFN-γ treatment either enhances the growth of serotonergic nerve fibers or was neuroprotective following SCI.

IFN-γ treatment increased the area of spared myelin

We performed Luxol fast blue (LFB) staining at 6 weeks post-SCI, and assessed the percentage of LFB-positive myelinated area relative to the total area of white matter. In both groups, the highest degree of demyelination occurred at the epicenter, and the area of spared myelin gradually increased rostrally and caudally (Fig. 8A). As shown in Figure 8B and C, IFN-γ treatment increased the myelinated area, and there was a significant difference between the two groups at 1.8 mm rostral and 0.6 mm caudal to the epicenter (Fig. 8A). The percentage of the myelinated area was 37.3 ± 1.5% in the vehicle-treated group, and 48.1 ± 1.6% in the IFN-γ-treated group, at 1.8 mm rostral to the epicenter, and 23.9 ± 2.0% in the vehicle-treated group, and 40.2 ± 2.6% in the IFN-γ-treated group, at 0.6 mm caudal to the epicenter (Fig. 8A). These data demonstrate that IFN-γ treatment increased the sparing of myelinated fibers post-SCI in mice.

IFN-γ treatment increased the expression of neurotrophic factors post-SCI

Since IFN-γ treatment increased the 5-HT-positive nerve fibers and enhanced sparing of myelinated fibers following SCI, we hypothesized that IFN-γ regulates the levels of certain neurotrophic factors post-SCI. We found that glial cell line-derived neurotrophic factor (GDNF) and insulin growth factor-1 (IGF-1) mRNA levels were significantly upregulated in the tissues surrounding the lesion epicenter in the IFN-γ-treated group, compared with those of the vehicle-treated group, whereas the levels of brain-derived neurotrophic factor (BDNF) and neurotrophin-3 (NT-3) mRNA were about the same in the two groups (Fig. 9A).

Discussion

In the present study, we demonstrated that IFN-γ exhibits therapeutic effects in an experimental mouse contusion SCI

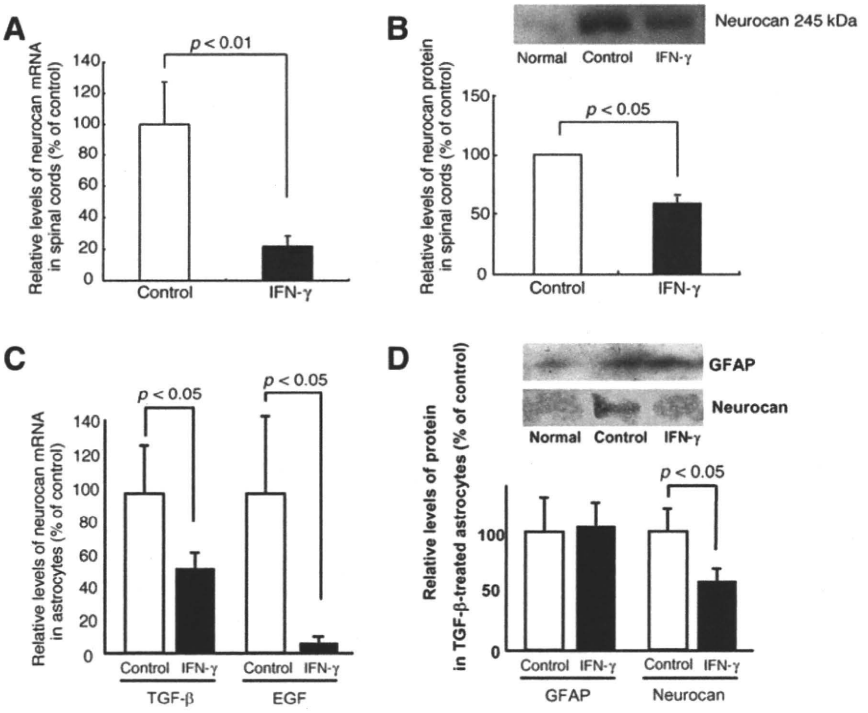

FIG. 6. Interferon-γ (IFN-γ) reduces chondroitin sulfate proteoglycan (CSPG) accumulation post-SCI. In order to analyze the levels of neurocan mRNA (**A**) and protein (**B**) in injured spinal cords with and without IFN-γ treatment, quantitative RT-PCR and Western blotting were performed ($n = 3$–6). (**C**) In the presence of TGF-β or EGF, cultured astrocytes were exposed to IFN-γ or vehicle (PBS) for 24 h, and the effects of IFN-γ on the levels of neurocan mRNA were analyzed by quantitative RT-PCR ($n = 3$–5). (**D**) TGF-β-treated astrocytes were exposed to IFN-γ or vehicle, protein was extracted, and Western blot analysis was performed to detect GFAP and neurocan. IFN-γ inhibited TGF-β-induced upregulation of neurocan protein expression (RT-PCR, real-time polymerase chain reaction; TFG-β, transforming growth factor-β; EGF, epidermal growth factor; GFAP, glial fibrillary acidic protein; SCI, spinal cord injury).

model, which is one of the clinically relevant animal models of SCI. To the best of our knowledge, this is the first study to demonstrate the therapeutic effects of IFN-γ on SCI. The IP administration of IFN-γ promoted significant functional recovery as early as 10 days post-SCI, suggesting that IFN-γ therapy could be valuable in the clinical setting. Notably, the hindlimbs of IFN-γ-treated mice displayed plantar stepping, whereas vehicle-treated mice could only move their ankles. In order to identify the anatomical basis for the functional recovery seen in IFN-γ-treated mice post-SCI, we initially attempted to trace the corticospinal tract by biotin dextran amine labeling; however, we were unable to obtain stable labeling in our mouse contusion SCI model. Therefore, we assessed the growth of 5-HT-positive raphe-spinal fibers, which are associated with locomotor recovery post-SCI (Kim et al., 2004). Consistent with the functional recovery seen in the IFN-γ-treated mice, we detected an increase in 5-HT-positive neuronal fibers following IFN-γ administration. In addition, we detected an increase in spared myelinated fibers in the white matter around the epicenter of the injured spinal cord in these mice. It has been reported that an increase in 5-HT-positive fibers and myelinated fibers strongly correlates with functional recovery post-SCI (Fouad et al., 2005; Kim et al., 2004; Oatway et al., 2005).

Although it remains to be determined how IFN-γ treatment promotes the growth of the neuronal axons and myelin sparing seen post-SCI, the decreased accumulation of axon growth inhibitors and increase in neurotrophic factors around the injured spinal cords in IFN-γ-treated mice may, at least partly, contribute to the enhanced restoration. In the present study, we found that IFN-γ treatment post-SCI significantly reduced the levels of CSPGs around the epicenter of injured spinal cords, with almost no effect on the number of reactive astrocytes, which are considered to be cellular sources of CSPGs. It is well established that the degradation of CSPGs by exogenously-administered chondroitinase ABC enhances histological and functional recovery post-SCI (Barritt et al., 2006; Bradbury et al., 2002). Therefore, it has been suggested that the IFN-γ-induced reduction of CSPG accumulation seen post-SCI creates an environment within the injured spinal cord that is conducive to axon growth. In addition to the immunohistochemical analyses, quantitative RT-PCR and Western blotting demonstrated that IFN-γ treatment suppressed the upregulation of neurocan mRNA and protein, which is one of CSPGs that is upregulated post-SCI, in injured spinal cords. This result suggests that IFN-γ treatment downregulates the levels of neurocan post-SCI at the transcriptional level. Consistent with this observation, neurocan mRNA in TGF-β- and EGF-treated astrocytes *in vitro* was significantly reduced by IFN-γ treatment (Fig. 6C), as has been demonstrated in previous studies (Asher et al., 2000; Smith and Strunz, 2005). In addition, IFN-γ inhibited the TGF-β-induced upregulation of neurocan protein

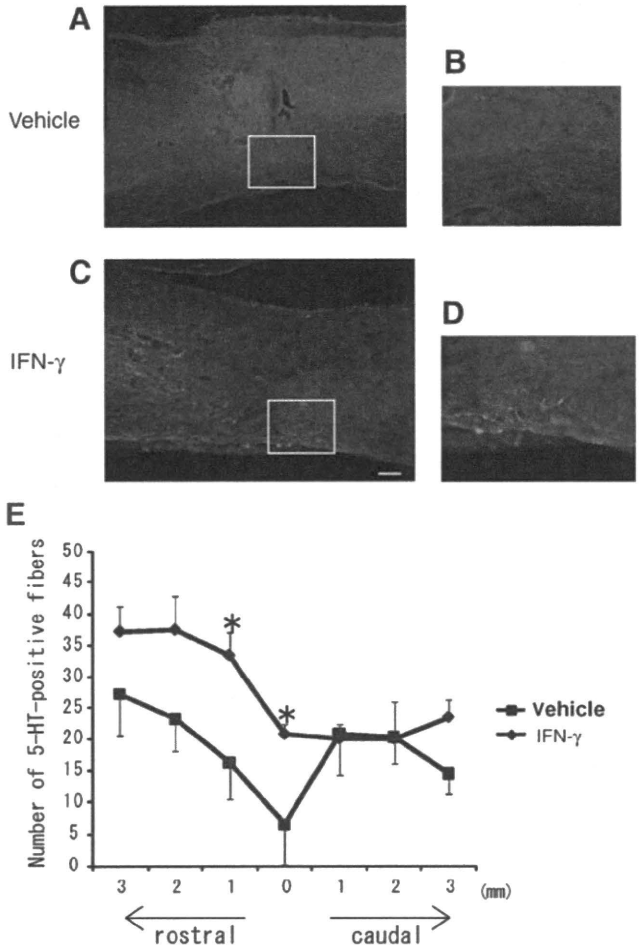

FIG. 7. Interferon-γ (IFN-γ) increases the number of 5-HT-positive fibers post-SCI. At 6 weeks post-SCI, the spinal cords of vehicle-treated (**A** and **B**) and IFN-γ-treated (**C** and **D**) mice were fixed, and sagittal sections were stained with anti-5-HT antibody. At the lesion center, higher-magnification images of the white boxes in **A** and **C** are shown in **B** and **D** (scale bar = 200 μm). (**E**) The numbers of 5-HT-positive fibers that crossed lines perpendicular to the central axis of the spinal cords were counted. The lines were positioned rostrally and caudally from the lesion center at 1-mm intervals. The number of 5-HT-positive fibers was significantly higher in IFN-γ-treated mice than in control mice at the lesion center and 1 mm rostral from the epicenter (*$p < 0.05$; 5-HT, serotonin; SCI, spinal cord injury).

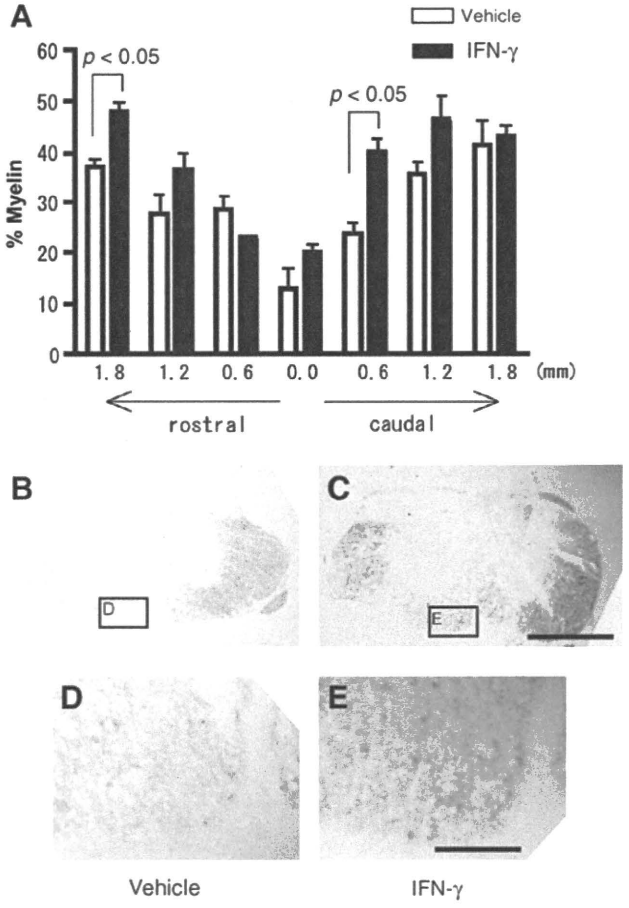

FIG. 8. Interferon-γ (IFN-γ) increases sparing of myelinated fibers post-SCI. At 6 weeks post-SCI, Luxol fast blue (LFB) staining of cross-sections of spinal cords was performed in order to analyze the effects of IFN-γ treatment on the levels of myelinated fibers seen post-SCI. (**A**) Graph showing the percentage of myelinated area relative to the total area of white matter in the cross-sections. We also assessed re-myelination or spared myelin by LFB staining in transverse sections. At least four samples, each at an 80-μm interval within 320 μm were isolated from the epicenter, and at 0.6 mm, 1.2 mm, and 1.8 mm rostral or caudal to the lesion epicenter. The number of myelinated fibers in the IFN-γ-treated group tended to be greater than in the control group, and the difference between the two groups at 1.8 mm rostral and 0.6 mm caudal from the center reached statistical significance ($p < 0.05$). (**B** and **C**) Representative LFB-stained cross sections at 400 μm caudal from the lesion center of vehicle-treated (**B** and **D**) and IFN-γ-treated (**C** and **E**) spinal cords are shown. The myelinated fibers were more dense in the IFN-γ-treated mice than in the vehicle-treated mice (SCI, spinal cord injury).

expression, whereas IFN-γ treatment had no influence on TGF-β-induced GFAP expression enhancement (Fig. 6D). GFAP upregulation is thought to be one of the manifestations of astrocyte activation. Thus IFN-γ treatment does not suppress the astrocyte activation itself, but suppresses CSPG upregulation. However, IFN-γ had no significant effect on EGF-induced neurocan upregulation. The precise mechanism underlying the discrepancy in the influence of IFN-γ between neurocan mRNA and protein expression in EGF-stimulated astrocytes is still unclear. These results suggest that IFN-γ treatment suppresses the upregulation of CSPGs at the transcriptional level post-SCI, by modulating the function of reactive astrocytes. The reduction of CSPGs by IFN-γ treatment in the injured spinal cord is relatively specific, since we observed that the levels of other axon growth inhibitors, such as semaphorin 3A and Nogo A, did not change with IFN-γ treatment.

IFN-γ also modulates the functions of macrophages/microglia post-SCI. We found that IFN-γ administration induced a widespread distribution of macrophages/microglia post-SCI. One possible mechanism by which IFN-γ alters macrophage/microglia distribution is via the IFN-γ-induced expression of chemokines such as IL-10, RANTES, and MCP-1,

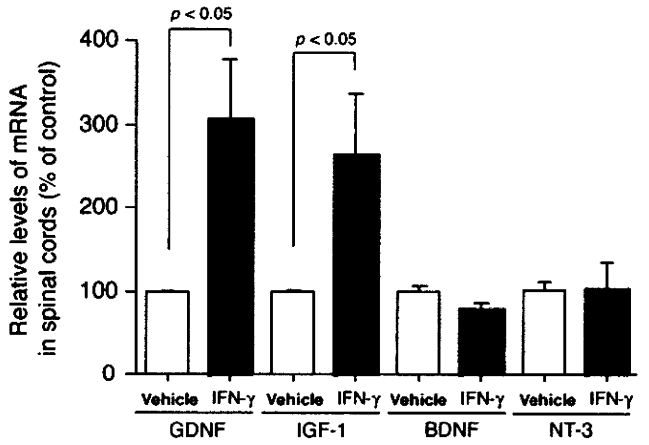

FIG. 9. Interferon-γ (IFN-γ) increases levels of neurotrophic factors post-SCI. The effects of IFN-γ on the expression levels of neurotrophic factors post-SCI were examined by quantitative RT-PCR for the indicated neurotrophic factors, as described in the legend to Figure 3 ($n = 3$; SCI, spinal cord injury; RT-PCR, real-time polymerase chain reaction; GDNF, glial cell line-derived neurotrophic factor (GDNF; IGF-1, insulin growth factor-1, BDNF, brain-derived neurotrophic factor; BNT-3, neurotrophin-3).

all of which promote the migration of macrophages into inflamed tissues (Schroder et al., 2004). In this context, we detected an upregulation of the mRNAs of MCP-1 and its receptor CCR2 in the IFN-γ-treated group at 7 days post-injury (Fig. 3E and F). Although the correlation between the IFN-γ-induced extensive accumulation of macrophages/microglia and the therapeutic effects of IFN-γ on SCI remain uncertain, the accumulation of macrophages/microglia induced by IFN-γ might produce effector molecules that support neuronal recovery post-SCI. Among these molecules, probable candidates for the promotion of neuronal recovery post-SCI are the IFN-γ-induced neurotrophic factors. It has been reported that activated macrophages/microglia produce several neurotrophic factors, such as NT-3, IGF-1, GDNF, and BDNF (Donnelly and Popovich, 2008; Elkabes et al., 1996; Hashimoto et al., 2005a, 2005b; Kaur et al., 2006; Nakajima et al., 2001). In this study, we detected an increase in the mRNAs of GDNF and IGF-1 with IFN-γ treatment post-SCI (Fig. 9). It is well established that these neurotrophic factors promote axon elongation and functional recovery post-SCI (Cheng et al., 2002; Grill et al., 1997; Iannotti et al., 2003; Sharma, 2005; Zhou et al., 2003). In this context, it has recently been proposed that IGF-1 is one of the axon-promoting factors of corticospinal motor neurons, the damage to which causes dysfunction of hindlimb movement in SCI models (Ozdinler and Macklis, 2006). In addition, these neurotrophic factors are reported to enhance the remyelination of PNS and CNS neuronal fibers in several experimental animal models (Blesch and Tuszynski, 2003; Girard et al., 2005; Mason et al., 2003; McTigue et al., 1998). These findings are consistent with our observation that IFN-γ treatment increases spared myelin post-SCI. At present, the cellular source of neurotrophic factors that are upregulated by IFN-γ treatment remains unclear. Our preliminary experiments showed that IFN-γ induces increased GDNF production by bone marrow-derived macrophages (BMDMs). In contrast, IFN-γ induced only a slight upregulation of GDNF expression by cultured microglia. Thus the main cellular source of GDNF may be macrophages. As for IGF-1, certain doses of IFN-γ can suppress IGF-1 expression in cultured microglia (Butovsky et al., 2006), and BMDMs. Therefore IFN-γ-mediated IGF-1 upregulation may be attributable to an interaction between IFN-γ-stimulated macrophages/microglia and the other cellular source within the spinal cord.

In the present study, we demonstrated that IFN-γ reduces the accumulation of CSPGs and enhances the production of GDNF and IGF-1 *in vivo* following SCI. Importantly, IFN-γ significantly promoted functional recovery following SCI in this experimental setting. The dose, timing, and duration of IFN-γ treatment should have a strong influence on its therapeutic effects. In a different setting, IFN-γ treatment might worsen the inflammatory reaction and exacerbate the paralysis resulting from SCI. Thus further exploration is needed to establish its optimal therapeutic regimen.

At present, the pharmacotherapeutic treatments available for human SCI are extremely limited. Since IFN-γ is currently used for the treatment of mycosis fungoides in humans, it would be of interest to test the therapeutic effects of clinically-available IFN-γ on patients with SCI.

Acknowledgments

We are grateful to Drs. T. Yamashita (Osaka University), and M. Hashimoto, Y. Someya, R. Kadota, C. Mannoji, T. Miyashita, J. Kawabe, T. Furuya, T. Endo, and K. Hayashi (Chiba University), for their helpful comments on this manuscript. This work was supported by a research grant from a Grant-in-Aid for Young Scientists (start-up) from Japan Society for the Promotion of Science (JSPS), and a research grant from the Futaba Electronics Memorial Foundation to T.K.

Author Disclosure Statement

No competing financial interests exist.

References

Asher, R.A., Morgenstern, D.A., Fidler, P.S., Adcock, K.H., Oohira, A., Braistead, J.E., Levine, J.M., Margolis, R.U., Rogers, J.H., and Fawcett, J.W. (2000). Neurocan is upregulated in injured brain and in cytokine-treated astrocytes. J. Neurosci. 20, 2427–2438.

Barritt, A.W., Davies, M., Marchand, F., Hartley, R., Grist, J., Yip, P., McMahon, S.B., and Bradbury, E.J. (2006). Chondroitinase ABC promotes sprouting of intact and injured spinal systems after spinal cord injury. J. Neurosci. 26, 10856–10867.

Blesch, A., and Tuszynski, M.H. (2003). Cellular GDNF delivery promotes growth of motor and dorsal column sensory axons after partial and complete spinal cord transections and induces remyelination. J. Comp. Neurol. 467, 403–417.

Bradbury, E.J., Moon, L.D., Popat, R.J., King, V.R., Bennett, G.S., Patel, P.N., Fawcett, J.W., and McMahon, S.B. (2002). Chondroitinase ABC promotes functional recovery after spinal cord injury. Nature 416, 636–640.

Butovsky, O., Ziv, Y., Schwartz, A., Landa, G., Talpalar, A.E., Pluchino, S., Martino, G., and Michal Schwartz, M. (2006). Microglia activated by IL-4 or IFN-γ differentially induce neurogenesis and oligodendrogenesis from adult stem/progenitor cells. Mol. Cell. Neurosci. 31, 149–160.

Cheng, H., Wu, J.P., and Tzeng, S.F. (2002). Neuroprotection of glial cell line-derived neurotrophic factor in damaged spinal cords following contusive injury. J. Neurosci. Res. 69, 397–405.

Deumens, R., Koopmans, G.C., and Joosten, E.A. (2005). Regeneration of descending axon tracts after spinal cord injury. Prog. Neurobiol. 77, 57–89.

Donnelly, D.J., and Popovich, P.G. (2008). Inflammation and its role in neuroprotection, axonal regeneration and functional recovery after spinal cord injury. Exp. Neurol. 209, 378–388.

Elkabes, S., DiCicco-Bloom, E.M., and Black, I.B. (1996). Brain microglia/macrophages express neurotrophins that selectively regulate microglial proliferation and function. J. Neurosci. 16, 2508–2521.

Fouad, K., Schnell, L., Bunge, M.B., Schwab, M.E., Liebscher, T., and Pearse, D.D. (2005). Combining Schwann cell bridges and olfactory-ensheathing glia grafts with chondroitinase promotes locomotor recovery after complete transection of the spinal cord. J. Neurosci. 25, 1169–1178.

Genovese, T., Mazzon, E., Crisafulli, C., Di Paola, R., Muià, C., Bramanti, P., and Cuzzocrea, S. (2006). Immunomodulatory effects of etanercept in an experimental model of spinal cord injury. J. Pharmacol. Exp. Ther. 316, 1006–1016.

Girard, C., Bemelmans, A.P., Dufour, N., Mallet, J., Bachelin, C., Nait-Oumesmar, B., Baron-Van Evercooren, A., and Lachapelle, F. (2005). Grafts of brain-derived neurotrophic factor and neurotrophin 3-transduced primate Schwann cells lead to functional recovery of the demyelinated mouse spinal cord. J. Neurosci. 25, 7924–7933.

Grill, R., Murai, K., Blesch, A., Gage, F.H., and Tuszynski, M.H. (1997). Cellular delivery of neurotrophin-3 promotes corticospinal axonal growth and partial functional recovery after spinal cord injury. J. Neurosci. 17, 5560–5572.

Hashimoto, M., Nitta, A., Fukumitsu, H., Nomoto, H., Shen, L., and Furukawa, S. (2005b). Inflammation-induced GDNF improves locomotor function after spinal cord injury. Neuroreport 16, 99–102.

Hashimoto, M., Nitta, A., Fukumitsu, H., Nomoto, H., Shen, L., and Furukawa, S. (2005a). Involvement of glial cell line-derived neurotrophic factor in activation processes of rodent macrophages. J. Neurosci. Res. 79, 476–487.

Iannotti, C., Li, H., Yan, P., Lu, X., Wirthlin, L., and Xu, X.M. (2003). Glial cell line-derived neurotrophic factor-enriched bridging transplants promote propriospinal axonal regeneration and enhance myelination after spinal cord injury. Exp. Neurol. 183, 379–393.

Jones, T.B., McDaniel, E.E., and Popovich, P.G. (2005). Inflammatory-mediated injury and repair in the traumatically injured spinal cord. Curr. Pharm. Des. 11, 1223–1236.

Kaur, C., Sivakumar, V., Dheen, S.T., and Ling, E.A. (2006). Insulin-like growth factor I and II expression and modulation in amoeboid microglial cells by lipopolysaccharide and retinoic acid. Neuroscience 138, 1233–1244.

Kigerl, K.A., McGaughy, V.M., and Popovich, P.G. (2006). Comparative analysis of lesion development and intraspinal inflammation in four strains of mice following spinal contusion injury. J. Comp. Neurol. 494, 578–594.

Kim, J.E., Liu, B.P., Park, J.H., and Strittmatter, S.M. (2004). Nogo-66 receptor prevents raphespinal and rubrospinal axon regeneration and limits functional recovery from spinal cord injury. Neuron 44, 439–451.

Koda, M., Nishio, Y., Kamada, T., Someya, Y., Okawa, A., Mori, C., Yoshinaga, K., Okada, S., Moriya, H., and Yamazaki, M. (2007). Granulocyte colony-stimulating factor (G-CSF) mobilizes bone marrow-derived cells into injured spinal cord and promotes functional recovery after compression-induced spinal cord injury in mice. Brain Res. 1149, 223–231.

Lazarov-Spiegler, O., Solomon, A.S., Zeev-Brann, A.B., Hirschberg, D.L., Lavie, V., and Schwartz, M. (1996). Transplantation of activated macrophages overcomes central nervous system regrowth failure. FASEB J. 10, 1296–1302.

Lee, Y.B., Yune, T.Y., Baik, S.Y., Shin, Y.H., Du, S., Rhim, H., Lee, E.B., Kim, Y.C., Shin, M.L., Markelonis, G.J., and Oh, T.H. (2000). Role of tumor necrosis factor-alpha in neuronal and glial apoptosis after spinal cord injury. Exp. Neurol. 166, 190–195.

Mason, J.L., Xuan, S., Dragatsis, I., Efstratiadis, A., and Goldman, J.E. (2003). Insulin-like growth factor (IGF) signaling through type 1 IGF receptor plays an important role in remyelination. J. Neurosci. 23, 7710–7718.

McKeon, R.J., Jurynec, M.J., and Buck, C.R. (1999). The chondroitin sulfate proteoglycans neurocan and phosphacan are expressed by reactive astrocytes in the chronic CNS glial scar. J. Neurosci. 19, 10778–10788.

McKeon, R.J., Schreiber, R.C., Rudge, J.S., and Silver, J. (1991). Reduction of neurite outgrowth in a model of glial scarring following CNS injury is correlated with the expression of inhibitory molecules on reactive astrocytes. J. Neurosci. 11, 3398–3411.

McTigue, D.M., Horner, P.J., Stokes, B.T., and Gage, F.H. (1998). Neurotrophin-3 and brain-derived neurotrophic factor induce oligodendrocyte proliferation and myelination of regenerating axons in the contused adult rat spinal cord. J. Neurosci. 18, 5354–5365.

Nakajima, K., Honda, S. Tohyama, Y., Imai, Y., Kohsaka, S., and Kurihara, T. (2001). Neurotrophin secretion from cultured microglia. J. Neurosci. Res. 65, 322–331.

Nesic, O., Xu, G.Y., McAdoo, D., High, K.W., High, K.W., Hulsebosch, C., and Perez-Pol, R. (2001). IL-1 receptor antagonist prevents apoptosis and caspase-3 activation after spinal cord injury. J. Neurotrauma 18, 947–956.

Nishio, Y., Koda, M., Kamada, T., Someya, Y., Kadota, R., Mannoji, C., Miyashita, T., Okada, S., Okawa, A., Moriya, H., and Yamazaki, M. (2007). Granulocyte colony-stimulating factor attenuates neuronal death and promotes functional recovery after spinal cord injury in mice. J. Neuropathol. Exp. Neurol. 66, 724–731.

Oatway, M.A., Chen, Y., Bruce, J.C., Dekaban, G.A., and Weaver, L.C. (2005). Anti-CD11d integrin antibody treatment restores normal serotonergic projections to the dorsal, intermediate, and ventral horns of the injured spinal cord. J. Neurosci. 25, 637–647.

Ozdinler, P.H., and Macklis, J.D. (2006). IGF-I specifically enhances axon outgrowth of corticospinal motor neurons. Nat. Neurosci. 9, 1371–1381.

Popovich, P.G., and Longbrake, E.E. (2008). Can the immune system be harnessed to repair the CNS? Nat. Rev. Neurosci. 9, 481–493.

Popovich, P.G., Wei, P., and Stokes, B.T. (1997). Cellular inflammatory response after spinal cord injury in Sprague-Dawley and Lewis rats. J. Comp. Neurol. 377, 443–464.

Rapalino, O., Lazarov-Spiegler, O., Agranov, E., Velan, G.J., Yoles, E., Fraidakis, M., Solomon, A., Gepstein, R., Katz, A., Belkin, M., Hadani, M., and Schwartz, M. (1998). Implantation of stimulated homologous macrophages results in partial recovery of paraplegic rats. Nat. Med. 4, 814–821.

Schroder, K., Hertzog, P.J., Ravasi, T., and Hume, D.A. (2004). Interferon-gamma: an overview of signals, mechanisms and functions. J. Leukoc. Biol. 75, 163–189.

Schwartz, M., Moalem, G., Leibowitz-Amit, R., and Cohen, I.R. (1999). Innate and adaptive immune responses can be beneficial for CNS repair. Trends. Neurosci. 22, 295–299.

Sharma, H.S. (2005). Neuroprotective effects of neurotrophins and melanocortins in spinal cord injury: an experimental study in the rat using pharmacological and morphological approaches. Ann. NY Acad. Sci. 1053, 407–421.

Shechter, R., London, A., Varol, C., Raposo, C., Cusimano, M., Yovel, G., Rolls, A., Mack, M., Pluchino, S., Martino, G., Jung, S., and Schwartz, M. (2009). Infiltrating blood-derived macrophages are vital cells playing an anti-inflammatory role in recovery from spinal cord injury in mice. PLoS Med. 6, e1000113.

Smith, G.M., and Strunz, C. (2005). Growth factor and cytokine regulation of chondroitin sulfate proteoglycans by astrocytes. Glia 52, 209–218.

Sroga, J.M., Jones, T.B., Kigerl, K.A., McGaughy, V.M., and Popovich, P.G. (2003). Rats and mice exhibit distinct inflammatory reactions after spinal cord injury. J. Comp. Neurol. 462, 223–240.

Stirling, D.P., Liu, S., Kubes, P., and Yong, V.W. (2009). Depletion of Ly6G/Gr-1 leukocytes after spinal cord injury in mice alters wound healing and worsens neurological outcome. J. Neurosci. 29, 753–764.

Yiu, G., and He, Z. (2006). Glial inhibition of CNS axon regeneration. Nat. Rev. Neurosci. 7, 617–627.

Zhou, L., Baumgartner, B.J., Hill-Felberg, S.J., McGowen, L.R., and Shine, H.D. (2003). Neurotrophin-3 expressed in situ induces axonal plasticity in the adult injured spinal cord. J. Neurosci. 23, 1424–1231.

Address correspondence to:
Masashi Yamazaki, M.D.
Department of Orthopaedic Surgery
Graduate School of Medicine
Chiba University
1-8-1 Inohana, Chuo-ku
Chiba 260-8677, Japan

E-mail: masashiy@faculty.chiba-u.jp

NEUROPATHOLOGY

Neuropathology 2010 doi:10.1111/j.1440-1789.2010.01130.x

Original Article

Transplantation of human bone marrow stromal cell-derived Schwann cells reduces cystic cavity and promotes functional recovery after contusion injury of adult rat spinal cord

Takahito Kamada,[1] Masao Koda,[4] Mari Dezawa,[5] Reiko Anahara,[2] Yoshiro Toyama,[3] Katsunori Yoshinaga,[6] Masayuki Hashimoto,[1] Shuhei Koshizuka,[1] Yutaka Nishio,[1] Chikato Mannoji,[1] Akihiko Okawa[1] and Masashi Yamazaki[1]

Departments of [1]Orthopaedic Surgery, [2]Bioenvironmental Medicine and [3]Anatomy and Developmental Biology, Chiba University Graduate School of Medicine, Chiba, [4]Department of Orthopaedic Surgery, Chiba Aoba Municipal Hospital, Chiba [5]Department of Stem Cell Biology and Histology, Tohoku University Graduate School of Medicine, Sendai, and [6]Chiba Rehabilitation Center, Chiba, Japan

The aim of this study was to evaluate whether transplantation of human bone marrow stromal cell-derived Schwann cells (hBMSC-SC) promotes functional recovery after contusive spinal cord injury of adult rats. Human bone marrow stromal cells (hBMSC) were cultured from bone marrow of adult human patients and induced into Schwann cells (hBMSC-SC) *in vitro*. Schwann cell phenotype was confirmed by immunocytochemistry. Growth factors secreted from hBMSC-SC were detected using cytokine antibody array. Immunosppressed rats were laminectomized and their spinal cords were contused using NYU impactor (10 g, 25 mm). Nine days after injury, a mixture of Matrigel and hBMSC-SC (hBMSC-SC group) was injected into the lesioned site. Five weeks after transplantation, cresyl-violet staining revealed that the area of cystic cavity was smaller in the hBMSC-SC group than that in the control group. Immunohistochemstry revealed that the number of anti-growth-associated protein-43-positive nerve fibers was significantly larger in the hBMSC-SC group than that in the control group. At the same time, the number of tyrosine hydroxylase- or serotonin-positive fibers was significantly larger at the lesion epicenter and caudal level in the hBMSC-SC group than that in the control group. In electron microscopy, formation of peripheral-type myelin was recognized near the lesion epicenter in the hBMSC-SC group. Hind limb function recovered significantly in the hBMSC-SC group compared with the control group. In conclusion, the functions of hBMSC-SC are comparable to original Schwann cells in rat spinal cord injury models, and are thus potentially useful treatments for patients with spinal cord injury.

Key words: axonal regeneration, bone marrow stromal cell, hind limb function, Schwann cell, spinal cord injury.

INTRODUCTION

It has been widely known that central and peripheral nervous systems show quite different reactions when they are injured. The former fails to regenerate, but the latter successfully regenerate their injured axons. The difference in the glial environment may be the key to the discrepancy in regenerating capacity between central and peripheral nervous systems. Oligodendrocytes form CNS myelin which contains inhibitory molecules for axonal regeneration, including myelin-associated glycoprotein, oligodendrocyte myelin glycoprotein and Nogo.[1] In contrast, Schwann cells, which form peripheral myelin, can express various types of neurotrophic factors and adhesion molecules, known to contribute to peripheral nervous system regeneration.[2] Thus, Schwann cells may have the capacity to convert the non-permissive environment for axonal regeneration of the CNS into a permissive one.[3] In fact, many researchers reported that transplantation of

Correspondence: Masao Koda, MD, PhD, Department of Orthopaedic Surgery, Chiba Aoba Municipal Hospital, 1273-2, Aoba-Cho, Chuo-Ku, Chiba 260-0852, Japan. Email: masaomst@yahoo.co.jp

Received 22 January 2010; revised and accepted 30 March 2010.

Schwann cells can promote axonal regeneration of lesioned adult rat spinal cord.[4]

Recently, we have reported that Schwann cells could be induced from bone marrow stromal cells *in vitro* (bone marrow stromal cell-derived Schwann cell; BMSC-SC) and they effectively promoted regeneration of lesioned sciatic nerves.[5,6] BMSC-SC can also promote axonal regeneration and functional recovery of hind limbs of completely transected[7] and contused[8] adult rat spinal cords, as we have reported previously. As a source of cell transplantation therapy for spinal cord injury, BMSC-SC has some advantages compared with original Schwann cells derived from peripheral nerves. First, BMSC can be easily obtained by bone marrow aspiration.[9] In contrast, harvesting Schwann cells from peripheral nerves needs to scarify the healthy peripheral nerve, resulting in complications including anesthesia or abnormal pain at the harvesting site. Bone marrow aspiration is much less invasive and can be performed in outpatient clinics. Second, BMSC is easily expanded *in vitro* because they can proliferate more vigorously than Schwann cells derived from peripheral nerves.[9] These advantages elevate BMSC-SC to a strong candidate for cell transplantation therapy for spinal cord injury. Recently we reported that human BMSC-SC (hBMSC-SC) can promote regeneration of transected rat sciatic nerves.[10] Thus there is a possibility that hBMSC-SC has a potential to promote hind limb functional recovery after spinal cord injury (SCI) as rat BMSC-SC promoted functional recovery after SCI, as we previously reported.

In the current study, we showed that hBMSC can be induced into Schwann cells characteristics *in vitro* and transplantation of hBMSC-SC reduced cystic cavity, promoted regeneration/sparing of several types of spinal cord axons and accelerated hind limb functional recovery in contusive spinal cord injury in adult rats.

MATERIALS AND METHODS

Human bone marrow stromal cell culture and hBMSC-SC induction *in vitro*

Human bone marrow stromal cells (hBMSC) were collected from a 22-year-old female patient during spinal surgery for benign spinal cord tumor (ependymoma in the conus medullalis region) with informed consent and accordance with the ethical committee of Chiba University Graduate School of Medicine. The cancellous bone in spinous processes was collected, minced and incubated with collagenase D (3 mg/mL, Roche Diagnostics, Basel, Switzerland) 37°C for 1 h to dislodge adherent cells.[11] Then the cells were washed with phosphate-buffered saline (PBS) three times and filtered. The filtered cells obtained from 0.5 mg of the original trabecular bone were plated onto 10-cm plastic dishes. Adherent cells were cultured as hBMSC with alpha-minimum essential Eagle medium (αMEM, Sigma, St Louis, MO, US) supplemented with 20% fetal bovine serum (FBS). Cells grown near confluence were treated with 0.25% trypsin (Sigma) and re-plated onto 10-cm plastic dishes at a split ratio of 1:3. BMSC at passage 1 were subjected to immunocytochemistry, transplantation experiments and Schwann cell induction.

Schwann cell induction was performed as previously described with minor modification.[5,7,10] In brief, hBMSC at passage 1 was incubated with αMEM containing 1 mM beta-mercaptoethanol for 24 h. After washing with PBS, medium was replaced with αMEM containing 10% FBS and 35 ng/mL all-*trans*-retinoic acid (Sigma) for 3 days. Cells were then transferred into αMEM containing 10% FBS, 5 μM forskolin (Calbiochem, La Jolla, CA, US), 10 ng/mL recombinant human basic fibroblast growth factor (Peprotech, London, UK), 5 ng/mL platelet derived-growth factor AB (Peprotech), and 200 ng/mL heregulin (R&D Systems, Minneapolis, MN, US) for 7 days.

To analyze the character of hBMSC and induced hBMSC-SC *in vitro*, we performed immunocytochemistry as previously described.[5,7] Anti-fibronectin (1:400; Chemicon, Temecula, CA, US) and anti-vimentin (1:400; DakoCytomation, Copenhagen, Denmark) were used as markers for marrow stromal cells. Anti-S-100 rabbit polyclonal antibody (S-100, 1:100; DakoCytomation), anti-p75 low affinity nerve growth factor receptor rabbit polyclonal antibody (p75LNGFR, 1:200; Chemicon) and anti-O4 mouse monoclonal antibody (1:400; Chemicon) were used as markers for Schwann cells. Cell nuclei were stained with 4′,6-diamidino-2-phenylindole (DAPI: Molecular Probes, Eugene, OR, US). The negative control was performed by omitting the primary antibodies.

To evaluate cytokines and growth factors secreted from hBMSC and hBMSC-SC, cytokine antibody array analysis was performed. hBMSC and hBMSC-SC were cultured in α-MEM without FBS in 5% CO_2 at 37°C for 24 h and the conditioned media were collected. Cytokines in the conditioned media of hBMSC and hBMSC-SC were investigated using the Human Cytokine Antibody Array® (RayBiotech, Inc., Norcross, GA, US) according to the manufacturer's instructions.

Spinal cord injury and transplantation

Tissue samples were obtained from 25 9-week-old male Wistar rats (average weight 200 g; SLC, Hamamatsu, Japan). Animals were anesthetized with 1.4–1.6% halothane in 1.5 L/min oxygen. Laminectomy was performed at the T9 level, leaving the dura intact. Then the spinal cord was contused with a 10 g weight rod dropped from 25 mm height using an NYU impactor at the T9 level.[12] Muscles

and skin were sutured layer to layer, and the rats placed in warm cages overnight. Manual bladder expression was performed twice a day until recovery of the bladder reflex.

One week after injury, the injured site was re-exposed and transplantation was performed. Mixture of Matrigel (BD Biosciences, Bedford, MA, US) and hBMSC-SC (hBMSC-SC group; 2×10^6 in 5 μL/rat, $n = 9$), Matrigel and hBMSC (hBMSC group; 2×10^6 in 5 μL/rat, $n = 9$) or Matrigel alone (MG group; 5 μL, $n = 7$) was injected into the injured site using a glass micropipette attached with a Hamilton microsyringe. We used Matrigel as a scaffold because Matrigel contains several kinds of extracellular matrices and growth factors and may promote survival of transplanted cells.

After transplantation, the T7 and T10 spinous processes were tied together tightly with a 1-0 silk suture to prevent kyphosis. Food and water were provided *ad libitum*. All the animals were given antibiotics in their drinking water (1.0 mL Bactramin (Roche) in 500 mL acidified water) for 2 weeks after transplantation.

All animals were immunosuppressed with cyclosporine A and dexamethasone. Twenty-four hours before transplantation, cyclosporine A (10 mg/kg) was injected subcutaneously. After transplantation, cyclosporine A was also injected for the entire experimental period (20 mg/kg on Monday and Wednesday, 40 mg/kg on Friday[13]). As an additional immunosuppressant, we used dexamethasone (0.5 mg/kg) 24 h before transplantation, and three times weekly during the first week post-transplantation.

None of the animals showed apparent abnormal behavior during the experimental period. All the experimental procedures were performed in compliance with the guidelines established by the Animal Care and Use Committee of Chiba University.

Tissue preparation

At the end of the functional assessment 6 weeks after injury, animals were perfused transcardially with 4% paraformaldehyde in PBS (pH 7.4) after an overdose of pentobarbital anesthesia. Three spinal cord segments (T8–10) including the injury epicenter were removed and post-fixed in the same fixative overnight, stored in 20% sucrose in PBS at 4°C and embedded in OCT (Sakura Finetechnical, Tokyo, Japan). Sagittal cryosections (20 μm in thickness) were mounted onto poly-L-lysine-coated slides (Matsunami, Tokyo, Japan).

Measurement of cystic cavity

To measure the area of the cystic cavity, every sixth section (120 μm apart) of the central portion of the spinal cords were selected. At least four samples from each animal were picked up, and thus the central 480 μm portion of the lesioned site was evaluated for cystic cavity. The sections were stained with cresyl-violet, dehydrated and sealed with Permount (Fisher Scientific, Fairlawn, NJ, US). We measured the area of the cystic cavity using Scion Image computer analysis software (Scion Corporation, Frederick, MA, US).

Immunohistochemistry

We performed immunohistochemistry as previously described.[7,14] The following primary antibodies were used to detect various types of nerve fibers: anti-growth-associated protein-43 (GAP-43, 1:400; Santa-Cruz Laboratories, Santa-Cruz, CA, US), anti-tyrosine hydroxylase monoclonal antibody (TH, 1:400; Chemicon), anti-serotonin rabbit polyclonal antibody (1:5000; Sigma) and anti-calcitonin gene-related peptide rabbit polyclonal antibody (CGRP, 1:1000; AFFINITI, Exeter, UK). After incubation with primary antibodies, the sections were incubated with Alexa 488-conjugated secondary anitibodies (Molecular Probes) to detect positive signals. We used GAP-43 as a general marker for regenerating/sprouting nerve fibers and the following markers for specific nerve fiber populations. TH-positive nerve fibers are mainly coerulo-spinal adrenergic nerve fibers and serotonin-positive nerve fibers are mainly raphe-spinal serotonergic fibers, both of which contribute to motor function.[15–18] To evaluate regeneration/sparing of GAP-43-, TH- or serotonin-positive nerve fibers, every sixth section was reacted with a specific antibody and the number of immunoreactive fibers that traversed the lines perpendicular to the central axis of the spinal cord at rostral (5 mm rostral to the injury epicenter), epicenter and caudal (5 mm caudal to epicenter) levels were counted in at least four samples from each animal; thus the central 480 μm portion of the graft was evaluated by immunohistochemistry.

To characterize transplanted cells, we performed a double immunofluorescence study for human cell-specific marker and cell-type markers 5 weeks after transplantation in the hBMSC and hBMSC-SC groups. Anti-human mitochondria mouse monoclonal antibody (1:100; Chemicon) was used as a marker for transplanted human-derived cells. Anti-fibronectin and anti-vimentin antibodies were used as markers for marrow stromal cells. Anti-S-100 and anti-p75 antibodies were used as markers for Schwann cells. Anti-microtuble-associated protein 2 antibody (MAP-2, 1:1000; Chemicon) was used as a marker for neurons, GFAP antibody (1:400; Sigma) was used as a marker for astrocytes and anti-myelin basic protein antibody (MBP, 1:200; Chemicon) was used as a marker for oligodendrocytes. After reaction with primary antibodies, sections were incubated with Alexa Fluor 488-conjugated anti-mouse IgG and Alexa Fluor 594-conjugated anti-

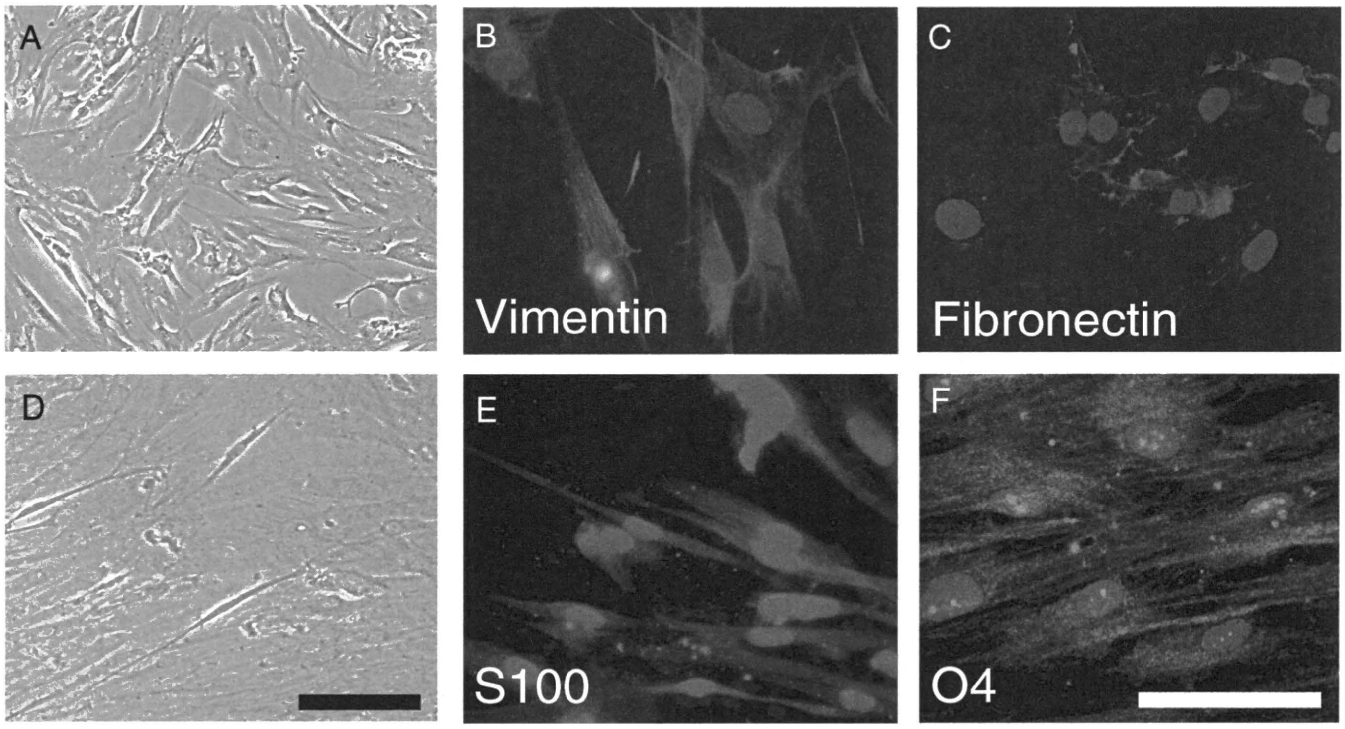

Fig. 1 (A) Phase-contrast microscopic image of human bone marrow stromal cells (hBMSC) cultured from cancellous bone. (B, C) Immunofluorescence of hBMSC for vimentin (B) and fibronectin (C). hBMSC was positive for vimentin and fibronectin. Nuclei were stained with 4′,6-diamidino-2-phenylindole (DAPI). (D) Phase-contrast microscopic image of Schwann cells induced from hBMSC (hBMSC-SC). The hBMSC-SC was morphologically and phenotypically similar to Schwann cells. (E, F) Immunofluorescence image of hBMSC-SC for S-100 (E) and O4 (F). hBMSC-SC was positive to S-100 or O4. Bars = 50 μm.

rabbit IgG (Molecular Probes). The fluorescent signals were observed by fluorescence microscopy (ECLIPSE E600; Nikon, Tokyo, Japan).

Electron microscopy

The rats were perfusion-fixed with 3% glutaraldehyde in HEPES ($C_8H_{18}O_4N_2S$) buffer (10 mM HEPES, 145 mM NaCl) under deep anesthesia. The spinal cord was excised, and part of the spinal cord including the injured site was immersion-fixed for an additional 90 min, after longitudinal slicing. The tissues were then post-fixed with 1% OsO4. After dehydration, the tissues were embedded in Epon. Semi-thin sections (1.5 μm) were stained with toluidine blue and precise areas for electron microscopy were selected and recorded under a light microscope. The semi-thin sections on the slide glass were re-embedded in Epon. Finally, ultra-thin sections from the precise areas were prepared and stained with uranyl acetate and lead citrate for electron microscopy (JEM 1200EX; JEOL, Tokyo, Japan).

Assessment of locomotor activity

Hind limb function of animals in all the groups was assessed using the BBB locomotor scale[19] before injury and 1 day, 3 days, and 1–6 weeks (once a week) after injury.

Statistics

All statistics were evaluated by multiple comparisons between groups. For histological studies, one-way analysis of variance (ANOVA) followed by Bonferroni/Dunn post-hoc test was used. For 6 weeks locomotor scale, repeated-measures ANOVA followed by Fisher's protected least significant difference (PLSD) post-hoc test was used. For fractional BBB score at eight time points, one-way ANOVA followed by Bonferroni/Dunn test was used. Differences were accepted for statistical significance at $P < 0.05$* and $P < 0.01$**.

RESULTS

Induced hBMSC-SC was apparently different in their morphology from that of original hBMSC. hBMSC showed fibroblast-like morphology but after induction they changed into spindle-shaped morphology similar to the Schwann cells (Fig. 1A,D). Immunocytochemistry showed that hBMSC was positive for fibronectin and vimentin (Fig. 1B,C) and induced hBMSC-SC was positive for S-100, O4 (Fig. 1E,F) and P75LNTFR (not shown), widely-known markers for Schwann cells. The percentage of cells positive for S-100, O4 and p75LNTFR after Schwann cell induction

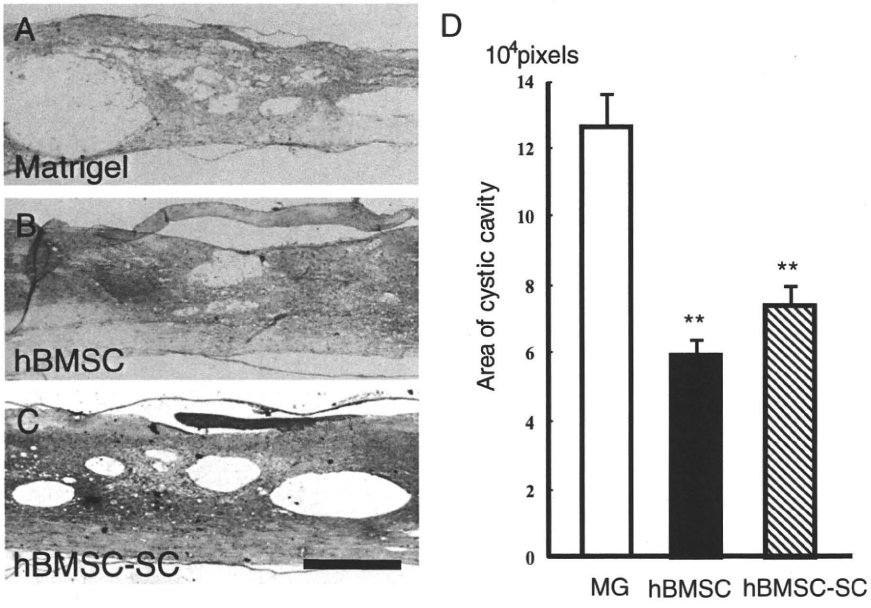

Fig. 2 Measurement of cystic cavity. The sections were stained with cresyl-violet. We measured the area of the cystic cavity using Scion Image computer analysis software. Arrows indicate the cystic cavity in the lesioned spinal cord. (A) In the Matrigel alone (MG) group, large cystic cavity formation was observed. (B, C) In the human bone marrow stromal cells (hBMSC) and Schwann cells induced from hBMSC (hBMSC-SC) groups, the area of cystic cavity was smaller than that of the MG group. (D) Statistical analysis of area of cystic cavity. In the hBMSC (closed column) and hBMSC-SC (hatched column) groups, the area of cystic cavity was significantly smaller than that of the MG group (open column). $*P < 0.01$. Bar = 1 mm in (A–C) and bars = ± SE in (D).

in vitro were all approximately 95%. Thus induced hBMSC-SC is morphologically and phenotypically identical to Schwann cells, as we described previously in rat BMSC.[7]

Next we performed cytokine assay using antibody array. The following factors were detected in hBMSC-SC-conditioned media: macrophage chemoattractant protein-1 (MCP-1), interleukin-6 (IL-6), insulin-like growth factor binding protein 2 and 4 (IGFBP-2 and 4), tissue inhibitor of metalloproteinase-1 and 2 (TIMP1 and 2) vascular endotherial growth factor (VEGF), urokinase receptor (uPAR), soluble tumor necrosis factor alpha receptor-1 (sTNF-αR) and interleukin-8 (IL-8) (Supporting Fig. S1).

Five weeks after transplantation, we measured the area of cystic cavity with cresyl violet staining (Fig. 2A–C). In the hBMSC (Fig. 2B,D, closed column) and hBMSC-SC (Fig. 2C,D, hatched column) groups, the average area of cystic cavity was significantly smaller than that in the MG group ($P < 0.01$; Fig. 2A,D, open column), indicating that transplantation of hBMSC or hBMSC-SC preserved spinal cord tissue. There was no significant difference between the hBMSC and hBMSC-SC groups in the cystic cavity area (Fig. 2D).

Next, we performed immunohistochemistry to evaluate axonal regeneration/sparing. The present results revealed that the number of GAP-43-positive nerve fibers at all three levels in the hBMSC-SC group was significantly larger than those in the MG and hBMSC groups ($P < 0.01$) (Figs 3A–C,4A). There was no significant difference between the MG and hBMSC groups in the number of GAP-43-positive nerve fibers at all three levels of the spinal cord (Fig. 4A).

To characterize the phenotype of regenerating/spared axons, we performed immunohistochemistry for nerve fiber markers. The numbers of TH-positive nerve fibers at the epicenter and caudal levels in the BMSC and hBMSC-SC groups were significantly larger than those in the MG group ($P < 0.01$) (Figs 3D–F, 4B). Furthermore, the number of TH-positive nerve fibers in the hBMSC-SC group was larger than that in the hBMSC group ($P < 0.05$; Fig. 4B). The number of serotonin-positive nerve fibers in the hBMSC and hBMSC-SC groups was apparently larger than that in the MG group at the epicenter and caudal levels ($P < 0.01$; Figs 3G–I, 4C). At the epicenter, the number of serotonin-positive nerve fibers was not statistically different between the hBMSC and hBMSC-SC groups. At the caudal level, the number of serotonin-positive fibers in the hBMSC-SC group was significantly larger than that in the hBMSC group ($P < 0.05$; Fig. 4C).

Double immunofluorescence study showed that almost all of human mitchondria-positive transplanted hBMSC were simultaneously positive for fibronectin or vimentin (not shown) and that all hBMSC-SC were also positive for S-100 (Fig. 5A–C, arrowhead) or p75LNGFR (not shown). The percentage of those indicating that transplanted hBMSC and hBMSC-SC maintained their specific phenotype observed *in vitro* even after transplantation. In addition, S100- or p75LNGFR-positive cells without human mitchondria immunoreactivity were observed around the lesioned site of the spinal cord (Fig. 5A–C), suggesting that endogenous Schwann cells migrated into the lesioned site. Those endogenous Schwann cells were also observed in the MG and hBMSC groups. There was no statistical difference in the number of endogenous Schwann cells between the groups (not shown). The number of human mitochondria-

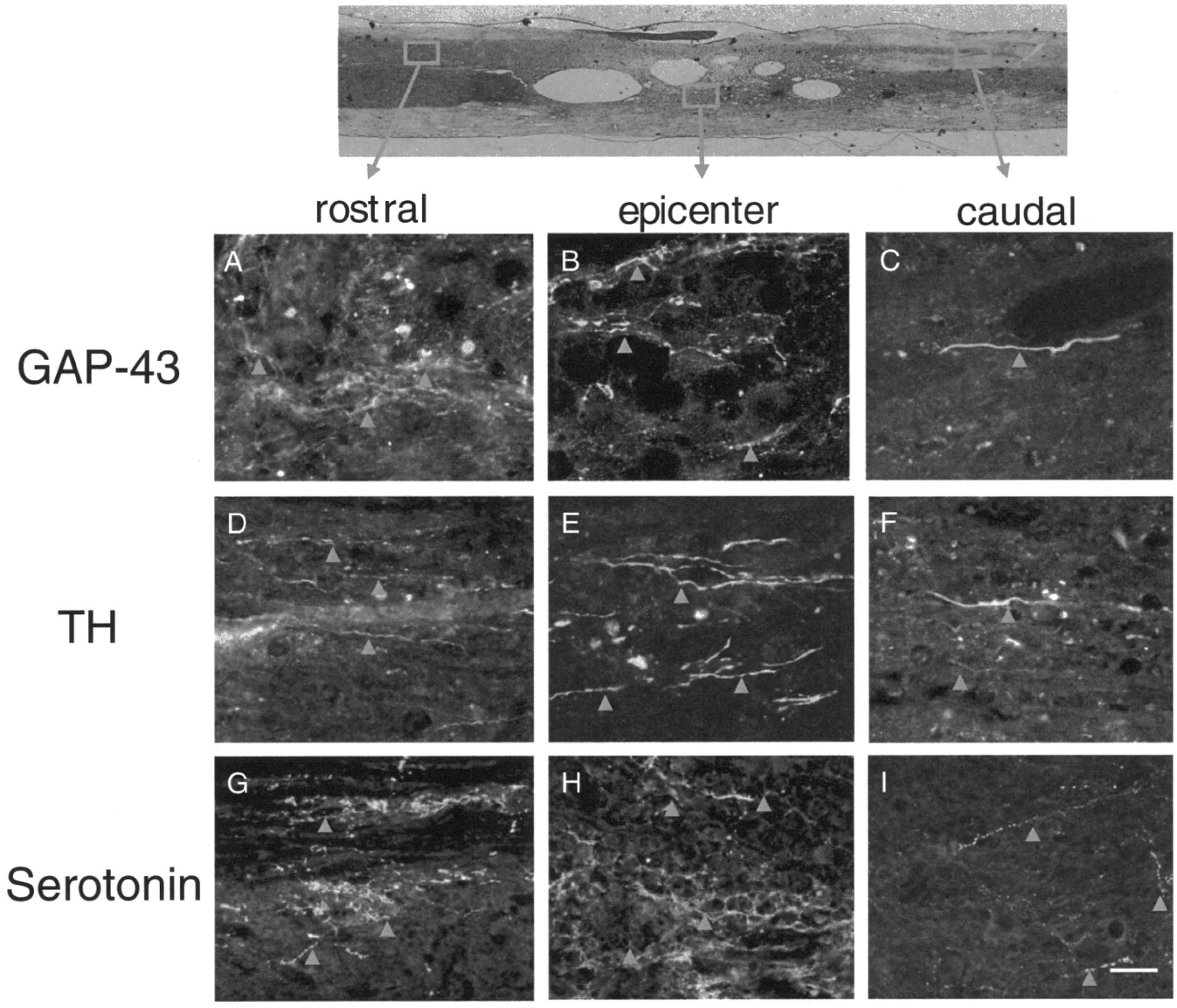

Fig. 3 Immunohistochemistry for nerve fiber markers in the Schwann cells induced from human bone marrow stromal cells (hBMSC-SC) group. Anti-growth-associated protein-43 (GAP-43)-positive fibers (A–C, arrowheads), tyrosine hydroxylase (TH) -positive fibers (D–F, arrowheads) and serotonin-positive fibers (G–I, arrowheads) were detected at the rostral, epicenter and caudal levels. Bar = 50 μm.

positive cells in the hBMSC and hBMSC-SC groups was 9.5 ± 2.0 and 10.2 ± 2.2 per section, respectively (not shown). There was no statistical difference in the number of human mitochondria-positive cells between the two groups. We could not detect cells that were double positive for human mitochondria and neural lineage markers (not shown).

In electron microscopic study of the hBMSC-SC group, myelin with basement membrane which is a specific feature of peripheral-type myelin formed by Schwann cells was observed near the lesioned site (Fig. 6A,B).

Finally, we assessed the recovery of hind limb function in all the three groups (Fig. 7). Hind limb function significantly recovered in both the hBMSC-SC ($P < 0.01$, Fig. 7, circle) and hBMSC ($P < 0.05$, Fig. 7, triangle) groups compared with the MG group (Fig. 7, square) from 4 weeks after transplantation, and a significant difference from the MG group was recognized up to 5 weeks after transplantation. The average recovery score in the hBMSC-SC group 5 weeks after transplantation was 11.7 ± 0.8, which indicates frequent to consistent weight-supported plantar steps and occasional fore limb–hind limb coordination, and recovery score in the hBMSC group was 10.5 ± 1.5, which indicates occasional weight-supported plantar steps without fore limb–hind limb coordination. There was no significant statistical difference between the hBMSC-SC

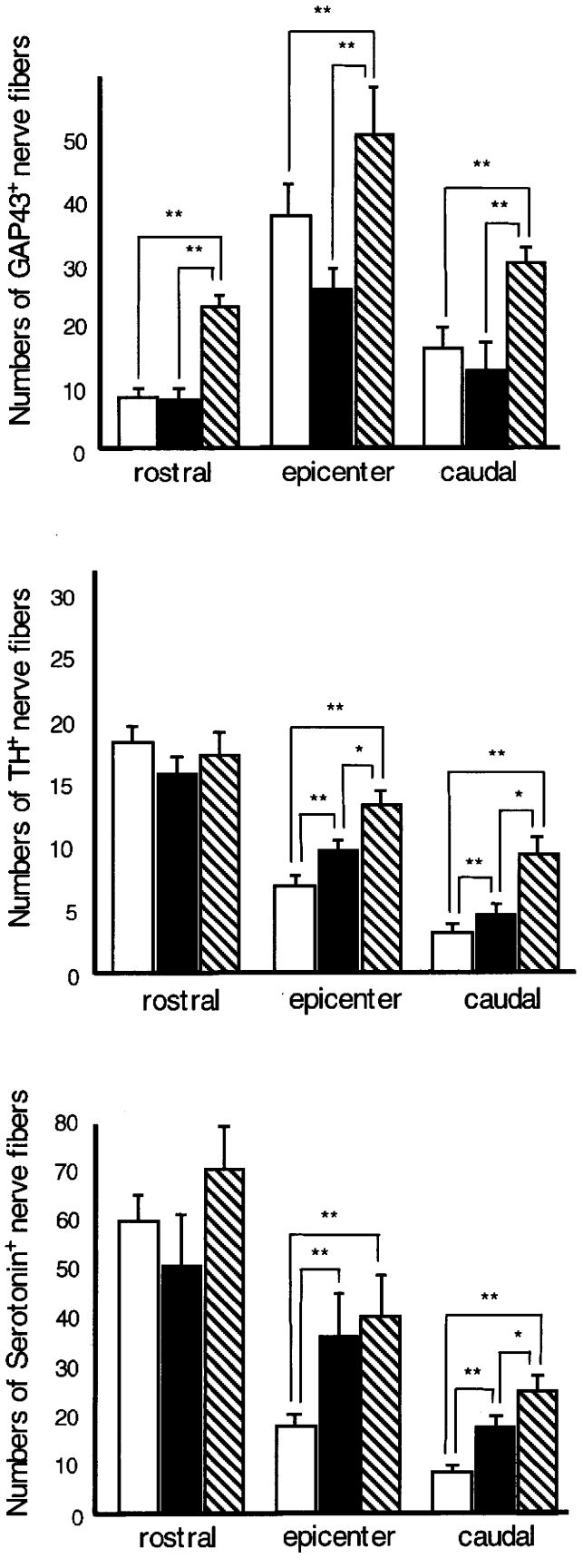

Fig. 4 Comparison of the average number of GAP-43-, tyrosine hydroxylase (TH)- and serotonin-positive fibers among the groups. Immunohistochemistry for anti-growth-associated protein-43 (GAP-43), TH and serotonin were performed and the number of immunoreactive fibers that traversed the lines perpendicular to the central axis of the spinal cord at rostral (5 mm rostral to the injury epicenter), epicenter and caudal (5 mm caudal to epicenter) levels were counted. The numbers of GAP-43-positive fibers were significantly larger in the Schwann cells induced from human bone marrow stromal cells (hBMSC-SC) group (A, hatched column) than those in the Matrigel alone (MG) (A, open column) and hBMSC (A, closed column) group at all three levels (**$P < 0.01$). The numbers of TH-positive fibers were significantly larger in the hBMSC (B, closed column) and hBMSC-SC (B, hatched column) groups than that in the MG group (B, open column) at the epicenter and caudal levels (**$P < 0.01$). Further, the numbers of TH-positive fibers in the hBMSC-SC group rats at the epicenter and caudal levels were significantly larger than that of the hBMSC group rats (*$P < 0.05$). The numbers of serotonin-positive fibers of the hBMSC (C, closed column) and hBMSC-SC (C, hatched column) groups were significantly larger than that of the MG group (open column) at the epicenter and caudal levels (**$P < 0.01$). There was no significant difference between the hBMSC and hBMSC-SC groups in the number of serotonin-positive fibers at all three levels. Closed columns: MG group; Open columns: BMSC-SC group. Bars = ± SE.

group and the hBMSC group in average BBB score at any time points. In the MG group, the average recovery score 5 weeks after transplantation was 7.67 ± 1.0, which indicates all three joints of hind limbs had extensive movement.

DISCUSSION

In the present study, transplantation of both hBMSC and hBMSC-SC reduced the cystic cavity and promoted modest axonal regeneration/sparing, which resulted in the recovery of hind limb function after contusive injury of the adult rat spinal cord. Transplantation of hBMSC-SC showed stronger axonal regeneration/sparing-promoting effect compared with hBMSC. We have already reported that BMSC-SC can promote axonal regeneration and functional recovery in a complete transaction model of adult rat spinal cord. For future clinical application, we need to prove the efficacy of the treatment for compression- or contusion-induced spinal cord injury, both of which are more relevant to clinical spinal cord injury than transection or hemisection models.[20] Thus we employed a contusive injury model using an NYU impactor, which is one of the gold standard models to study spinal cord injury treatment, and could successfully prove the efficacy of hBMSC-SC transplantation for that model.

Possible explanations of functional recovery obtained by transplantation of hBMSC-SC are as follows. First, hBMSC-SC has neuroprotective effects. Correlation

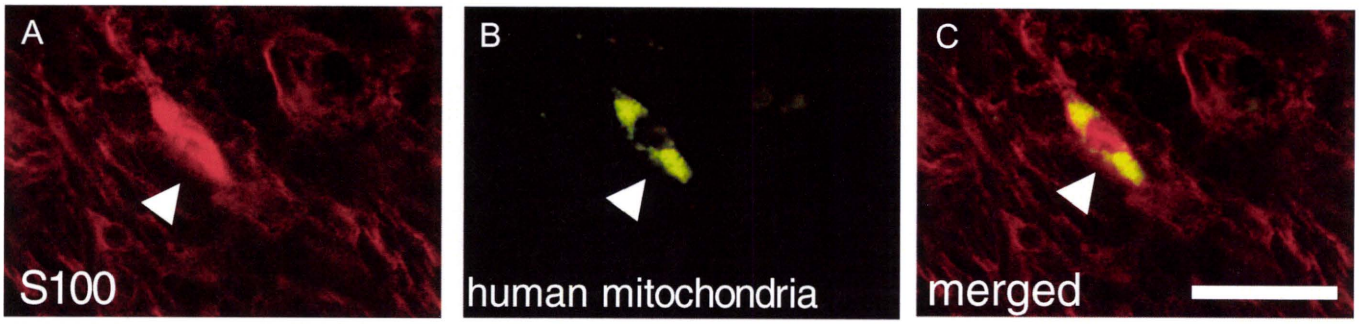

Fig. 5 Double immunofluorescence study for cell marker in the Schwann cells induced from human bone marrow stromal cells (hBMSC-SC) group 5 weeks after transplantation. (A) S-100 (B) human mitchondria (C) merged view; arrowhead indicates S-100 and human mitchondria double-positive cell. Bar = 50 μm.

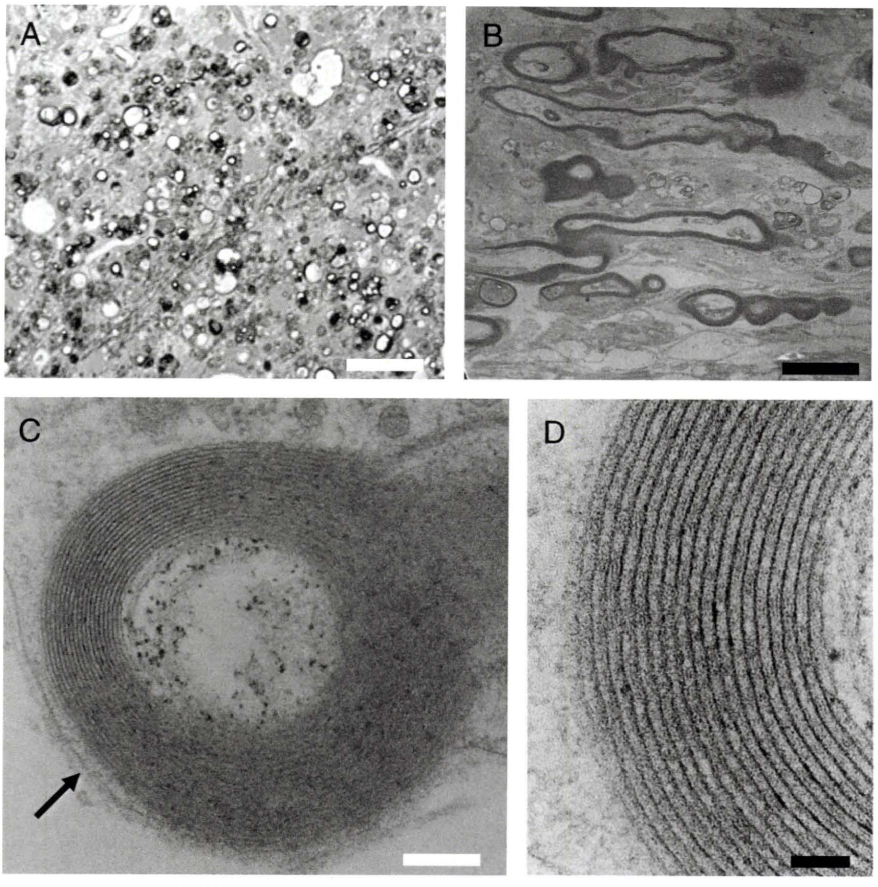

Fig. 6 Electron microscopic findings in the Schwann cells induced from bone marrow stromal cells (BMSC-SC) group. (A) Photomicrograph of Epon-embedded semi-thin transverse sections stained with toluidine blue. (B) Lower-magnification view and (C, D) higher-magnification views. (A, B) Large numbers of myelin sheaths were observed near the injured site. (C, D) Higher-magnification image revealing lamellar formation with basement membrane, which is characteristic of peripheral-type myelin (arrow in (C)). Bars = 10 μm in (A), 1 μm in (B), 500 nm in (C) and 100 nm in (D).

between the reduction of cystic cavity volume and hind limb functional recovery has been reported.[21–23] Thus the reduction of the area of cystic cavity reflects spinal cord tissue sparing, reflecting neuroprotective effects of the treatment. The present results showed that transplantation of hBMSC-SC significantly reduced the area of cystic cavity, showing the neuroprotective property of hBMSC-SC. Second, hBMSC-SC has a potential to enhance axonal regeneration similar to those of rat BMSC-SC.[7,8] The present results showed that transplantation of hBMSC-SC increased the number of GAP-43-positive fibers at the lesioned site and the adjacent sites. Similarly, hBMSC-SC increased the number of TH- and serotonin-positive fibers at the caudal site in contused adult rat spinal cord, both descending fibers of which contribute to motor function.[15–18] GAP-43-positive fibers may include not only regenerating fibers but also local sprouting. TH-positive fibers may include not only descending fibers but also peripheral fibers derived from sympathetic nerves as well.[24] Thus it is hard to distinguish between regenerating central

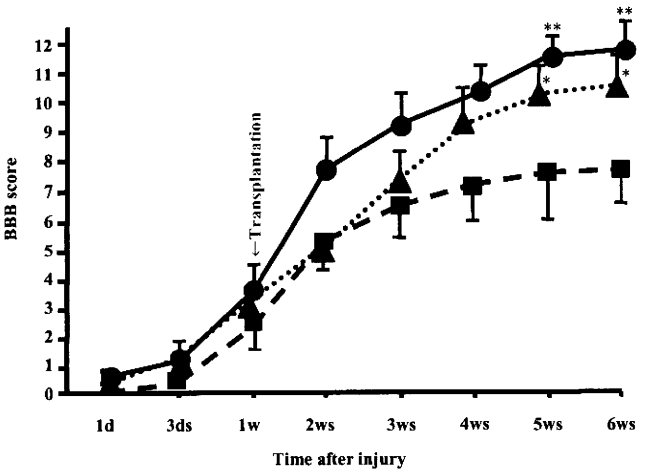

Fig. 7 Hind limb functional recovery. Hind limb function recovered significantly in the Schwann cells induced from human bone marrow stromal cells (hBMSC-SC) (triangle, $*P < 0.05$) and hBMSC-SC (square, $**P < 0.01$) groups from 4 weeks after transplantation, and a significant difference from the Matrigel alone (MG) group (circle) was maintained until 5 weeks after transplantation. The average recovery score in the hBMSC group was 10.5, which indicates occasional weight-supported plantar steps without fore limb–hind limb coordination, and the average recovery score in the hBMSC-SC group was 11.7, which indicates frequent and consistent weight-supported plantar steps and occasional fore limb–hind limb coordination, whereas that in the MG group it was 7.67, which indicates all three joints of hind limbs had extensive movement. $*P < 0.05$ and $**P < 0.01$. Bars = ± SE.

axons from local sprouting and/or peripheral-derived axons. However, recent reports showed that local sprouting can contribute to functional recovery.[25,26] Therefore, the increased number of several types of nerve fibers might associate with functional recovery.

In the present study, injured rats showed a tendency to recover at a relatively early stage after transplantation of transplanted cells, and also only a small number of transplanted cells survived in the injured spinal cord. Thus, it is more likely that the soluble factors secreted from transplanted hBMSC-SC influenced the course of improvement than that integration of transplanted cells into host neural circuit contributes to functional recovery. Our hypothesis is supported by the recent findings that BMSC can secrete several neurotrophic factors and these factors would have the potential to work effectively toward the recovery of spinal cord injury.[9,27,28] To elucidate the soluble factors secreted from hBMSC-SC, we performed cytokine antibody array. The results of cytokine antibody array revealed that several kinds of growth factors are potentially neurotrophic. For example, VEGF is known to suppress secondary degeneration and promote functional recovery after spinal cord injury,[29] TIMP-1 and 2 were reported to suppress the apoptosis of neurons[30] and TIMP-2 has been reported to promote neurite outgrowth of PC-12 cells.[31]

In addition to these mechanisms, hBMSC-SC may enhance re-myelination as shown by the findings of electronic microscopy in the present study. The fact that only a few hBMSC-SC could survive in the lesioned spinal cord suggests that transplantation of hBMSC-SC promoted migration of endogenous Schwann cells into the lesioned site and they re-myelinated axons in the injured spinal cord together with the transplanted hBMSC-SC.[32]

We suggest that one of the possible merits of Schwann cell induction is the promotion of survival after transplantation into the lesioned spinal cord, which was shown in our previous report.[8] However, the present results showed that only a small number of transplanted hBMSC-SC could survive in the injured spinal cord regardless of immunosuppression. Immunological rejection may occur for certain xeno-grafted cells. We expect if the transplanted hBMSC-SC could survive and integrate into lesioned spinal cord, axonal regeneration and functional recovery might be more obviously accelerated.

The principal findings of the present study were that hBMSC-SC could be successfully induced from hBMSC and they could restore injured spinal cord tissue in the contusion injury model. Although more precise characterization of hBMSC-SC is needed, the present results showed that hBMSC-SC is morphologically and phenotypically identical to Schwann cells. It encourages us to step forward hBMSC-SC transplantation for clinical application that hBMSC-SC has a potential to restore lesioned spinal cord.

In conclusion, transplantation of Schwann cells derived from bone marrow stromal cells is a potentially useful treatment for spinal cord injury. Although further exploration is needed to establish optimal conditions for more effective functional recovery, our study advances us toward using cell transplantation therapy for treatment of spinal cord injury.

ACKNOWLEDGMENTS

This work was supported by grants-in-aid for Scientific Research from the Ministry of Education, Science and Culture of Japan (16390427) and by a grant from the General Insurance Association of Japan.

REFERENCES

1. Profylis C, Cheema SS, Zang DW. Degenerative and regenerative mechanisms governing spinal cord injury. *Neurobiol Dis* 2004; **15**: 415–436.
2. Bunge MB. Bridging areas of injury in the spinal cord. *Neuroscientist* 2001; **7**: 325–339.
3. Jones LL, Oudega M, Bunge MB, Tsuzynski MH. Neurotrophic factors, cellular bridges and gene therapy for spinal cord injury. *J Physiol* 2001; **533**: 83–89.

4. Bunge MB, Pearse DD. Transplantation strategies to promote repair of the injured spinal cord. *J Rehabil Res Dev* 2003; **40**: 55–62.
5. Dezawa M, Takahashi I, Esaki M, Takano M, Sawada H. Sciatic nerve regeneration in rats induced by transplantation of *in vitro* differentiated bone-marrow stromal cells. *Eur J Neurosci* 2001; **14**: 1771–1776.
6. Mimura T, Dezawa M, Kanno H, Sawada H, Yamamoto I. Peripheral nerve regeneration by transplantation of bone marrow stromal cell-derived Schwann cells in adult rats. *J Neurosurg* 2004; **101**: 806–812.
7. Kamada T, Koda M, Dezawa M *et al.* Transplantation of bone marrow stromal cell-derived Schwann cells promotes axonal regeneration and functional recovery after complete transection of adult rat spinal cord. *J Neuropathol Exp Neurol* 2005; **64**: 37–45.
8. Someya Y, Koda M, Dezawa M *et al.* Reduction of cystic cavity, promotion of axonal regeneration and sparing, and functional recovery with transplanted bone marrow stromal cell–derived Schwann cells after contusion injury to the adult rat spinal cord. *J Neurosurg Spine* 2008; **9**: 600–610.
9. Chopp M, Li Y. Treatment of neural injury with marrow stromal cells. *Lancet Neurol* 2002; **1**: 92–100.
10. Shimizu S, Kitada M, Ishikawa H, Itokazu Y, Wakao S, Dezawa M. Peripheral nerve regeneration by the in vitro differentiated-human bone marrow stromal cells with Schwann cell property. *Biochem Biophys Res Commun* 2007; **359**: 915–920.
11. Sakaguchi Y, Sekiya I, Yagishita K, Ichinose S, Shinomiya K, Muneta T. Suspended cells from trabecular bone by collagenase digestion become virtually identical to mesenchymal stem cells obtained from marrow aspirates. *Blood* 2004; **104**: 2728–2735.
12. Young W. Spinal cord regeneration. *Science* 1996; **273**: 450–451.
13. Wennersten A, Meier X, Holmin S, Wahlberg L, Mathiesen T. Proliferation, migration, and differentiation of human neural stem/progenitor cells after transplantation into a rat model of traumatic brain injury. *J Neurosurg* 2004; **100**: 88–96.
14. Hashimoto M, Koda M, Ino H, Murakami M, Yamazaki M, Moriya H. Upregulation of osteopontin expression in rat spinal cord microglia after traumatic injury. *J Neurotrauma* 2003; **20**: 287–296.
15. Bregman BS, Kunkel-Bagden E, Reier PJ, Dai HN, McAtee M, Gao D. Recovery of function after spinal cord injury: mechanisms underlying transplant-mediated recovery of function differ after spinal cord injury in newborn and adult rats. *Exp Neurol* 1993; **123**: 3–16.
16. Deumans R, Koopmans GC, Joosten EAJ. Regeneration of descending axon tracts after spinal cord injury. *Prog Neurobiol* 2005; **77**: 57–89.
17. Shapovalov AI. Neuronal organization and synaptic mechanisms of supraspinal motor control in vertebrates. *Rev Physiol Biochem Pharmacol* 1975; **72**: 1–54.
18. Villanueva L, Bernard JF, Le Bars D. Distribution of spinal cord projections from the medullary subnucleus reticularis dorsalis and the adjacent cuneate nucleus: a *Phaseolus vulgaris*-leucoagglutinin study in the rat. *J Comp Neurol* 1995; **352**: 11–32.
19. Basso DM, Beattie MS, Bresnahan JC. A sensitive and reliable locomotor rating scale for open field testing in rats. *J Neurotrauma* 1995; **12**: 1–21.
20. Steeves JD, Fawcett JW, Tuszynski M. Report of international clinical trials workshop on spinal injury. Feb 20–21 2004, Vancouver Canada. *Spinal Cord* 2004; **42**: 591–597.
21. Gorio A, Madaschi L, Di Stefano B *et al.* Methylprednisolone neutralizes the beneficial effects of erythropoietin in experimental spinal cord injury. *Proc Natl Acad Sci USA* 2005; **102**: 16379–16384.
22. Ohta M, Suzuki Y, Noda T *et al.* Bone marrow stromal cells infused into the cerebrospinal fluid promote functional recovery of the injured rat spinal cord with reduced cavity formation. *Exp Neurol* 2004; **187**: 266–278.
23. Wu S, Suzuki Y, Ejiri Y *et al.* Bone marrow stromal cells enhance differentiation of cocultured neurosphere cells and promote regeneration of injured spinal cord. *J Neurosci Res* 2003; **72**: 343–351.
24. Chung K, Chung JM. Sympathetic sprouting in the dorsal root ganglion after spinal nerve ligation: evidence of regenerative collateral sprouting. *Brain Res* 2001; **895**: 204–212.
25. Bareyre FM, Kerschensteiner M, Raineteau O, Mettenleiter TC, Weunmann O, Schwab ME. The injured spinal cord spontaneously forms a new intraspinal circuit in adult rats. *Nat Neurosci* 2004; **7**: 269–277.
26. Courtine G, Song B, Roy RR *et al.* Recovery of supraspinal control of stepping via indirect propriospinal relay connections after spinal cord injury. *Nat Med* 2008; **14**: 69–74.
27. Chen Q, Long Y, Yuan X *et al.* Protective effects of bone marrow stromal cell transplantation in injured rodentbrain: synthesis of neurotrophic factors. *J Neurosci Res* 2005; **80**: 611–619.
28. Chen X, Katakowski M, Li Y *et al.* Human bone marrow stromal cell cultures conditioned by traumatic brain tissue extracts: growth factor production. *J Neurosci Res* 2002; **69**: 687–691.

29. Widenfalk J, Lipson A, Jubran M *et al.* Vascular endotherial growth factor improves functional outcome and decreases secondary degeneration in experimental spinal cord contusion injury. *Neuroscience* 2003; **120**: 951–960.
30. Gardner J, Ghorpade A. Tissue inhibitor of metalloproteinase (TIMP)-1: the TIMPed balance of matrix metalloproteinases in the central nervous system. *J Neurosci Res* 2003; **74**: 801–806.
31. Pérez-Martínez L, Jaworski DM. Tissue inhibitor of metalloproteinase-2 promotes neuronal differentiation by acting as an anti-mitogenic signal. *J Neurosci* 2005; **25**: 4917–4929.
32. Baron-Van Evercooren A, Avellana-Adalid V, Lachapelle F, Liblau R. Schwann cell transplantation and myelin repair of the CNS. *Mult Scler* 1997; **3**: 157–161.

SUPPORTING INFORMATION

Additional Supporting Information may be found in the online version of this article:

Fig. S1 Cytokine array analysis of hBMSC-SC-conditioned media. hBMSC-SC-conditioned media was incubated with cytokine antibody arrays following manufacturer's instruction (RayBio® human cytokine antibody array 6 and 7 (RayBiotech, Inc., Norcross, GA, US). The following factors were detected in hBMSC-SC-conditioned media: macrophage chemoattractant protein-1 (MCP-1), interleukin-6 (IL-6), insulin-like growth factor binding protein 2 and 4 (IGFBP-2 and 4), tissue inhibitor of metalloproteinase-1 and 2 (TIMP1 and 2) vascular endotherial growth factor (VEGF), urokinase receptor (uPAR), soluble tumor necrosis factor alpha receptor-1 (sTNF-αR) and interleukin-8 (IL-8) (Supporting Fig. S1). Positive control spots were indicated by asterisks.

Please note: Wiley-Blackwell are not responsible for the content or functionality of any supporting materials supplied by the authors. Any queries (other than missing material) should be directed to the corresponding author for the article.

SPINE Volume 33, Number 24, pp 2648–2650

Radiographic Predictors for the Development of Myelopathy in Patients With Ossification of the Posterior Longitudinal Ligament

A Multicenter Cohort Study

Shunji Matsunaga, MD, PhD,* Kozo Nakamura, MD, PhD,† Atsushi Seichi, MD, PhD,† Toru Yokoyama, MD, PhD,‡ Satoshi Toh, MD, PhD,‡ Shoichi Ichimura, MD, PhD,§ Kazuhiko Satomi, MD, PhD,§ Kenji Endo, MD, PhD,¶ Kengo Yamamoto, MD, PhD,¶ Yoshiharu Kato, MD, PhD,‖ Tatsuo Ito, MD, PhD,‖ Yasuaki Tokuhashi, MD, PhD,** Kenzo Uchida, MD, PhD,†† Hisatoshi Baba, MD, PhD,†† Norio Kawahara, MD, PhD,‡‡ Katsuro Tomita, MD, PhD,‡‡ Yukihiro Matsuyama, MD, PhD,§§ Naoki Ishiguro, MD, PhD,§§ Motoki Iwasaki, MD, PhD,¶¶ Hideki Yoshikawa, MD, PhD,¶¶ Kazuo Yonenobu, MD, PhD,‖‖ Mamoru Kawakami, MD, PhD,*** Munehito Yoshida, MD, PhD,*** Shinsuke Inoue, MD, PhD,††† Toshikazu Tani, MD, PhD,††† Kazuo Kaneko, MD, PhD,‡‡‡ Toshihiko Taguchi, MD, PhD,‡‡‡ Takanori Imakiire, MD,* and Setsuro Komiya, MD, PhD§§§

Study Design. A multicenter cohort study was performed retrospectively.

Objective. To identify radiographic predictors for the development of myelopathy in patients with ossification of the posterior longitudinal ligaments (OPLL).

Summary of Background Data. The pathomechanism of myelopathy in the OPLL remains unknown. Some patients with large OPLL have not exhibited myelopathy for a long periods of time. Predicting the course of future neurologic deterioration in asyptomatic patients with OPLL is difficult at their initial visit.

Methods. A total of 156 OPLL patients from 16 spine institutes with an average of 10.3 years of follow-up were reviewed. Subjects underwent a plain roentgenogram, computed tomography (CT), and magnetic resonance imaging of the cervical spine during the follow-up. The trauma history of the cervical spine, maximum percentage of spinal canal stenosis in a plain roentgenogram and CT, range of motion of the cervical spine, and axial ossified pattern in magnetic resonance imaging or CT were reviewed in relation to the existence of myelopathy.

Results. All 39 patients with greater than 60% spinal canal stenosis on the plain roentgenogram exhibited myelopathy. Of 117 patients with less than 60% spinal canal stenosis, 57 (49%) patients exhibited myelopathy. The range of motion of the cervical spine was significantly larger in patients with myelopathy than in those of without it. The axial ossified pattern could be classified into 2 types: a central type and a lateral deviated type. The incidence of myelopathy in patients with less than 60% spinal canal stenosis was significantly higher in the lateral deviated-type group than in the central-type group. Fifteen patients of 156 subjects developed trauma-induced myelopathy. Of the 15 patients, 13 had mixed-type OPLL and 2 had segmental-type OPLL.

Conclusion. Static and dynamic factors were related to the development of myelopathy in OPLL.

Key words: OPLL, myelopathy, CT, dynamic factor.
Spine 2008;33:2648–2650

From the *Department of Orthopaedic Surgery, Imakiire General Hospital, Kagoshima; †Department of Orthopaedic Surgery, Faculty of Medicine, University of Tokyo, Tokyo; ‡Department of Orthopaedic Surgery, Hirosaki University, Graduate School of Medicine, Aomori; §Department of Orthopaedic Surgery, Kyorin University School of Medicine, Tokyo; ¶Department of Orthopaedic Surgery, Tokyo Medical University; ‖Department of Orthopaedic Surgery, Tokyo Women's Medical University, Tokyo; **Department of Orthopaedic Surgery, Nihon University School of Medicine, Tokyo; ††Department of Orthopaedics and Rehabilitation Medicine, Faculty of Medicine, Fukui University, Fukui; ‡‡Department of Orthopaedic Surgery, Faculty of Medical Science, Kanazawa University, Ishikawa; §§Department of Orthopaedic Surgery, Nagoya University School of Medicine, Aichi; ¶¶Department of Orthopaedic Surgery, Osaka University Graduate School of Medicine, Osaka; ‖‖Department of Orthopaedic Surgery, National Hospital Osaka South Medical Center, Osaka; ***Department of Orthopaedic Surgery, Wakayama Medical University, Wakayama; †††Department of Orthopaedic Surgery, Kochi Medical School, Kochi; ‡‡‡Department of Orthopaedic Surgery, Yamaguchi Graduate University School of Medicine, Yamaguchi; and §§§Department of Orthopaedic Surgery, Graduate School of Medical and Dental Sciences, Kagoshima University, Kagoshima Prefecture, Japan.

Acknowledgment date: January 10, 2008. First revision date: March 5, 2008. Second revision date: March 18, 2008. Acceptance date: March 20, 2008.

The manuscript submitted does not contain information about medical device(s)/drug(s).

Other funds (The Investigation Committee on the Ossification of Spinal Ligaments of the Japanese Ministry of Health, Labor, and Welfare) were received in support of this work. No benefits in any form have been or will be received from a commercial party related directly or indirectly to the subject of this manuscript.

This study was performed with the aid of the Investigation Committee on the Ossification of the Spinal Ligaments of the Japanese Ministry of Health, Labor, and Welfare.

This study was performed with the approval of the Clinical Research Ethics Committee of each institute.

Address correspondence and reprint requests to Shunji Matsunaga, MD, PhD, Department of Orthopaedic Surgery, Imakiire General Hospital, 4–16, Shimotastuo chou, Kagoshima 892-8502, Japan; E-mail: shunji@m.kufm.kaqgoshima-u.ac.jp

The pathomechanism of myelopathy in ossification of the posterior longitudinal ligament (OPLL) remains unknown. Therefore, it is difficult to predict the course of future neurologic deterioration in patients with OPLL. We designed a multicenter cohort study to identify the